

GR-87-3

HYDRAULIC MODEL STUDY OF ENLARGED SPILLWAY FOR PACTOLA DAM

May 1987
Engineering and Research Center



U.S. Department of the Interior
Bureau of Reclamation
Division of Research and
Laboratory Services
Hydraulics Branch

TECHNICAL REPORT STANDARD TITLE PAGE

1. REPORT NO. GR-87-3	2. GOVERNMENT ACCESSION NO.	3. RECIPIENT'S CATALOG NO.	
4. TITLE AND SUBTITLE Hydraulic Model Study of Enlarged Spillway for Pactola Dam		5. REPORT DATE May 1987	
		6. PERFORMING ORGANIZATION CODE D-1531	
7. AUTHOR(S) P. L. Johnson		8. PERFORMING ORGANIZATION REPORT NO. GR-87-3	
9. PERFORMING ORGANIZATION NAME AND ADDRESS Bureau of Reclamation Engineering and Research Center Denver, CO 80225		10. WORK UNIT NO.	
		11. CONTRACT OR GRANT NO.	
12. SPONSORING AGENCY NAME AND ADDRESS Same		13. TYPE OF REPORT AND PERIOD COVERED	
		14. SPONSORING AGENCY CODE DIBR	
15. SUPPLEMENTARY NOTES Microfiche and/or hard copy available at the E&R Center, Denver, Colorado <p style="text-align: right;">Editor:RNW(c)</p>			
16. ABSTRACT Recent hydrologic studies of Pactola Dam, South Dakota, and its drainage have yielded a substantially increased maximum design flood. To safely handle the increased flood, the dam will be raised 15 feet (4.6 m) and the spillway widened from 240 to 425 feet (73 to 130 m). With these modifications, the maximum spillway discharge capacity will be 245,000 ft ³ /s (6940 m ³ /s). A 1:60 scale physical model was used to develop and verify the hydraulic design of an enlarged unlined open chute spillway for this existing dam. The study concentrated on evaluating tailwater velocity and wave action as a function of discharge, of tailwater elevation, and of scour and deposition influences. Of particular interest was the resulting hydraulic action on the dam embankment face. The model indicated that for discharges of 200,000 ft ³ /s (5660 m ³ /s) or greater, the hydraulic jump would sweep out of the proposed unlined stilling basin. It was concluded that velocities as high as 15 to 20 ft/s (4.6 to 6.1 m/s) and corresponding trough-to-crest short-period wave heights as great as 4.5 feet (1.4 m) could occur on the embankment face. In addition, a discharge rating curve for the spillway was developed, and reservoir approach velocities to the spillway crest and their potential for erosion were evaluated.			
17. KEY WORDS AND DOCUMENT ANALYSIS a. DESCRIPTORS-- spillways/ model tests/ hydraulics/ hydraulic structures/ spillway crest/ discharge coefficients/ stilling basins/ embankments/ erosion b. IDENTIFIERS-- Pactola Dam, South Dakota/ Missouri Basin Region c. COSATI Field/Group COWRR: SRIM:			
18. DISTRIBUTION STATEMENT		19. SECURITY CLASS (THIS REPORT) UNCLASSIFIED	21. NO. OF PAGES 43
		20. SECURITY CLASS (THIS PAGE) UNCLASSIFIED	22. PRICE

GR-87-3

**HYDRAULIC MODEL STUDY
OF ENLARGED SPILLWAY
FOR PACTOLA DAM**

by

P. L. Johnson

Hydraulics Branch
Division of Research
and Laboratory Services
Engineering and Research Center
Denver, Colorado

May 1987



ACKNOWLEDGMENTS

The studies were conducted by the author with assistance from C. A. States. They were conducted under the direct supervision of T. J. Rhone, Head, Hydraulic Structures Section, with general supervision and review from P. H. Burgi, Chief, Hydraulics Branch, and D. D. Daniels, Principal Designer, Concrete Dams Branch. The assistance of D. G. Achterberg, Concrete Dams Branch, and W. W. Childs and W. I. Jones, both from the laboratory shops, greatly aided in the completion of this study.

As the Nation's principal conservation agency, the Department of the Interior has responsibility for most of our nationally owned public lands and natural resources. This includes fostering the wisest use of our land and water resources, protecting our fish and wildlife, preserving the environmental and cultural values of our national parks and historical places, and providing for the enjoyment of life through outdoor recreation. The Department assesses our energy and mineral resources and works to assure that their development is in the best interests of all our people. The Department also has a major responsibility for American Indian reservation communities and for people who live in Island Territories under U.S. Administration.

CONTENTS

	Page
Purpose and application	1
Introduction.....	1
Conclusions	2
The model	4
The investigation.....	6
Appendix.....	12

FIGURES

Figure

1	General plan of Pactola Dam and spillway.....	15
2	Location map	17
3	Hydraulic model, 1:60 scale	18
4	Fixed bed model scour hole.....	19
5	Fixed bed tailwater velocity distribution for discharge of 62,500 ft ³ /s (1770 m ³ /s).....	20
6	Fixed bed tailwater velocity distribution for discharge of 125,000 ft ³ /s (3540 m ³ /s).....	21
7	Fixed bed tailwater velocity distribution for discharge of 187,000 ft ³ /s (5310 m ³ /s).....	22
8	Fixed bed tailwater velocity distribution for discharge of 245,000 ft ³ /s (6940 m ³ /s).....	23
9	Fixed bed hydraulic model at various discharges	24
10	Fixed bed, long-period maximum observed wave amplitudes	25
11	Fixed bed, short-period (2- to 4-s) maximum observed wave amplitudes	26
12	Influence of high tailwater on fixed bed flow for discharge of 245,000 ft ³ /s (6940 m ³ /s).....	27
13	Model with erodible bed	28
14	Operation of model with erodible bed at various discharges	29
15	Erodible bed tailwater velocity distribution for discharge of 62,500 ft ³ /s (1770 m ³ /s).....	30
16	Erodible bed tailwater velocity distribution for discharge of 125,000 ft ³ /s (3540 m ³ /s).....	31
17	Erodible bed tailwater velocity distribution for discharge of 187,500 ft ³ /s (5310 m ³ /s).....	32
18	Erodible bed tailwater velocity distribution for discharge of 245,000 ft ³ /s (6940 m ³ /s)	33
19	Erodible bed scour at various discharges.....	34
20	Point erosion with deposition bar for discharge of 245,000 ft ³ /s (6940 m ³ /s)	35
21	Erodible bed maximum observed wave amplitudes over point.....	36
22	End contraction of flow at crest	37
23	Crest discharge coefficients from 1:60 and 1:36 scale models.....	38
24	Discharge rating curve	39
25	Topography at spillway intake (2 sheets).....	41
26	Velocity distribution in reservoir approach to spillway for discharge of 245,000 ft ³ /s (6940 m ³ /s)	43

PURPOSE AND APPLICATION

The studies were made to refine and confirm the hydraulic performance of an enlarged spillway for Pactola Dam, South Dakota. Of particular interest were the tailwater flow patterns and resulting erosion that were associated with the substantially increased spillway discharge. It was felt that such erosion might endanger the dam embankment.

The results of this model study have only limited application at other sites. Tailwater flow and erosion patterns are strongly dependent on structure and topography configuration as well as on discharge, head differential, and tailwater depth. Because all of these parameters tend to be site-specific, the observed flow and erosion patterns are also site-specific. For a location with similar arrangement and topography, the findings from this study may give insight into the flow conditions.

Other hydraulic aspects of the design, such as the adequacy of the approach to the crest, the discharge coefficient of the crest, and the adequacy of the chute to contain the maximum discharge, were all evaluated. These items are also strongly dependent on site-specific topography. This is particularly evident when it is noted that little excavation was done to upgrade the approach to the crest and that high ground on the left (looking in the direction of flow) approaching the crest will probably influence crest performance. Note also that the chute is an excavated unlined feature whose grade and sidewall heights are dictated by the existing topography. Consequently, direct application of these findings to other sites is limited.

INTRODUCTION

Pactola Dam (fig. 1) is a 230-foot (70-m) high earthfill structure located on Rapid Creek about 15 miles (24 km) west of Rapid City, South Dakota (fig. 2). The reservoir provides irrigation water, much of the domestic water for Rapid City, and flood protection along Rapid Creek. The reservoir has an active capacity of 55,000 acre-feet (6.8×10^7 m³) and a total capacity of 99,000 acre-feet (1.2×10^8 m³). The dam has an excavated unlined spillway in the left abutment with a 240-foot (73-m) long uncontrolled concrete crest and a design capacity of 38,400 ft³/s (1090 m³/s).

Recent hydrologic studies have yielded a substantially increased maximum design flood. To safely handle this flood, the dam will be raised 15 feet (4.6 m) and the spillway widened from 240 feet (73 m) to 425 feet (130 m). With these modifications, the maximum spillway discharge capacity will be increased from 38,400 ft³/s (1090 m³/s) to 245,000 ft³/s (6940 m³/s). With the wider spillway, the maximum unit discharge (discharge per unit width of crest) will increase by a factor of approximately 3.6.

The model study was conducted to evaluate various hydraulic features of the modified design. There was particular concern that the increased discharge would create back eddies or wave action that could erode the toe of the dam. It was thought that at the higher discharges, the modified spillway stilling basin would probably be inadequate and would sweep out. This would yield high-velocity flow that would cross the valley and impinge on the opposite hillside. A portion of the flow would then be deflected upstream toward the embankment. In addition, a shear zone would occur between the outflow from the stilling basin and the portion of the tailwater pool located between the outflow and the dam. It was thought that the combination of these factors could cause a strong eddy that could erode the dam embankment. Thus, the potential erosion and the resulting downstream deposition caused by both flow velocity and wave action were of primary interest in the study. Spillway approach flow conditions, discharge rating, and flow conditions on the chute were also evaluated.

CONCLUSIONS

1. Tailwater flow velocities on the modeled dam embankment face were evaluated for numerous operating conditions. The velocities were determined for spillway discharges of 62,500, 125,000, 187,500, and 245,000 ft³/s (1770, 3540, 5310, 6940 m³/s) with both fixed and erodible tailwater topography. The erodible topography included 5-foot (1.5-m) deep overburden on all flow surfaces, an erodible point between the outlet works and spillway stilling basins, and a fixed scour hole filled with erodible material at the toe of the spillway chute. In addition, velocities were observed with the tailwater elevations set at levels predicted by theoretical analysis and at levels that might correspond to conditions resulting from downstream deposition of scoured materials. In all cases, the maximum observed velocities along the dam embankment face occurred at the maximum discharge. With fixed topography, the point located between the spillway and the outlet works (fig. 1) tended to isolate the spillway flow from the dam embankment. Consequently, fixed topography velocities along the dam face were minimal; the maximum observed velocities were approximately 1.0 ft/s (0.3 m/s) (fig. 8). With the fixed topography, velocities observed with the tailwater artificially elevated an additional 10 feet (3.0 m) were less than those observed with the lower tailwater (fig. 12). These reduced velocities were attributed to additional energy dissipation resulting from the higher tailwater and to the increased cross-sectional area of flow. With the erodible bed, formation of a shallow scour hole and a downstream deposition bar was noted at a discharge of 62,500 ft³/s (1770 m³/s) (fig. 19). At 125,000 ft³/s (3540 m³/s), scour had progressed to the extent of the hypothesized scour hole (which had been set as fixed topography in the model) (fig. 19), and the downstream channel had been swept free of overburden and deposition. At this discharge, flow over the point between the two stilling basins had started to erode the point (fig. 20). Erosion of the point increased the area of influence of the spillway flow.

The design requires that waste or excavated material from the enlarged spillway be placed in a waste pile immediately downstream of the dam embankment. At 125,000 ft³/s (3540 m³/s), this waste pile totally isolates the tailwater flow from the embankment (fig. 16). At 187,500 ft³/s (5310 m³/s), erosion of downstream overburden continued to expand, the downstream channel was swept free of deposition, a large bar continued to grow to the right and downstream of the spillway stilling basin, scour of the point between the stilling basins progressed, and erosion continued on the waste pile, which still isolated the embankment from the tailwater flow (fig. 10). Finally, at 245,000 ft³/s (6940 m³/s), the scour of the point, of the waste pile, and of the general overburden reached their maximum (fig. 19); the downstream channel remained clear of deposition; a large deposition bar was present to the right and downstream of the spillway stilling basin; and the tailwater was high enough to submerge the waste piles by approximately 5 feet (1.5 m). Thus, there was direct exposure of the dam embankment to tailwater action. Observed velocities along the embankment were less than 10 ft/s (3.0 m/s) (fig. 18). Velocities as high as 15 to 20 ft/s (4.6 to 6.1 m/s) were observed along the waste pile face. The velocities observed with the erodible topography and with the tailwater artificially elevated an additional 10 feet (3.0 m/s) were less than the velocities observed at the lower tailwater.

2. Wave action, the other potential cause of erosion of the dam embankment, was monitored over the same range of operating conditions as the velocities. Wave data were collected along surfaces surrounding the point, the embankment, and the waste pile. Two frequencies of waves were noted. With the fixed bed, long-period surging was observed in the embayment between the point and the dam. Observed surge periods ranged from 62 to 93 seconds. Maximum trough-to-crest wave magnitudes of up to 5.4 feet (1.65 m) were noted (fig. 10). These maximum long-period waves were observed with a spillway discharge of 187,500 ft³/s (5310 m³/s). In addition, shorter-period (11- to 15-s) surges were noted at the point, and maximum trough-to-crest amplitudes of up to 7.5 feet (2.3 m) occurred at 245,000 ft³/s (6940 m³/s) (fig. 10). Superimposed on these surges were short-period (2- to 4-s) waves. At the dam, the maximum amplitude of the short-period waves was from 3.3 to 4.5 feet (1.0 to 1.4 m) (fig. 11). Maximum amplitudes occurred at discharges of either 187,500 or 245,000 ft³/s (5310 or 6940 m³/s). Over the point, the maximum amplitude of short-period waves, approximately 4.7 feet (1.4 m), occurred at a discharge of 245,000 ft³/s (6940 m³/s) (fig. 11). Because of the extremely long surge period at the dam embankment, the short-period wave amplitudes represent the critical dynamic loading on the dam face. Over the point, the surge period is much shorter and, consequently, the surge amplitude can compound the dynamic loading of the short-period waves and yield short-period through-to-crest amplitudes of up to approximately 12 feet (3.7 m). It should be noted that the top of the point is at approximately elevation 4436.0 (1352.1 m) and, consequently, the tailwater surface with its wave action tends to be above the point for the higher discharges. The erosion influences of the

wave action should therefore be reduced. As with velocity, artificially elevated tailwater yielded increased energy dissipation and reduced wave amplitudes.

In the erodible bed model, observed wave amplitudes were lower than those for the fixed bed model. No surging was noted near the embankment. A large-diameter eddy rotated over the point with maximum trough-to-crest wave heights of 5 feet (1.5 m) (fig. 21). Short-period wave action on the dam embankment was minimal.

3. The proposed waste pile placement at the downstream toe of the dam (fig. 1) will supply substantial protection of the dam embankment from tailwater flows. By placing it to elevation 4450.0 feet (1356.4 m), the waste pile will extend above the tailwater surface for all but the largest discharges.

4. The model indicates that hydraulic forces are dominant and that bar deposition in the downstream channel, which could raise tailwater elevations, will not occur. All of the topography that could influence tailwater elevation was included in the model. Nevertheless, potential influences of elevated tailwater were evaluated. As previously noted, it was found that artificially elevated tailwater yielded increased energy dissipation and reduced tailwater velocities and wave action.

5. The model data indicate that the maximum discharge of 245,000 ft³/s (6940 m³/s) can be passed with a reservoir water surface elevation of 4651.7 feet (1417.8 m). Discharge coefficients from this 1:60 model were compared with corresponding coefficients from a 1:36 sectional model previously studied (fig. 23). The coefficients were found to compare closely over the mid-discharge range. The 1:60 model shows lower coefficients at higher discharges. This is due to end contractions that could not occur in the 1:36 sectional model. A crest discharge rating (fig. 24) based on the 1:60 model and crest discharge coefficients as a function of reservoir water surface elevation (fig. 23) were derived.

6. Maximum spillway approach velocities occurred at the maximum discharge of 245,000 ft³/s (6940 m³/s). Maximum observed approach velocities over the fill or dike surface (which might be susceptible to erosion) were approximately 12 ft/s (3.7 m/s). Velocities of this magnitude were observed in localized areas near the crest (fig. 26). Local velocities as high as 25 to 30 ft/s (7.6 to 9.1 m/s) were noted in the spillway approach channel and in the approach flow end contractions (fig. 22).

THE MODEL

The hydraulic model (fig. 3) used in this study was constructed at a scale of 1:60. Included in the model were an approximately 500- by 1,000-foot (150- by 300-m) prototype area of reservoir topography immediately surrounding the spillway intake, the spillway crest and chute, and an

approximately 1,100- by 1,600-foot (340- by 490-m) prototype area of topography below the dam and spillway. The reservoir topography modeled was adequate to properly represent the topographic influence on the approach flow to the crest. The head box was large enough and the topography was installed in such a manner that box influences on the approach flow distribution were minimized. Enough downstream topography was included to ensure that all topographic influences on the flow, including natural channel control of water surface elevations, were represented.

Because the spillway chute is unlined and, consequently, relatively rough, friction losses on the chute were thought to be potentially significant. Chute losses could influence resulting flow velocities, stilling basin sweepout, and thus, the general flow patterns downstream from the dam. Therefore, extra care was taken to correctly represent the chute surface. Observation of the existing chute showed the typical roughness element heights to be 0.5 foot (0.2 m). With this roughness height, roughness element height-to-flow depth ratios (relative roughness) may be as small as 0.019 on portions of the chute at maximum discharge. Geometric scaling of roughness heights will yield correctly represented losses for a relative roughness of 0.019 if model Reynolds numbers are greater than 4×10^4 at the maximum discharge. Calculations indicate that with the 1:60 scale, model Reynolds numbers at the 245,000-ft³/s (6940-m³/s) discharge will be approximately 1×10^5 . Therefore, it was concluded that geometric scaling of roughness would yield correctly represented losses. The model chute was constructed with the 0.5-foot (0.15-m) prototype roughness heights scaled to 0.10 inch (2.5 mm). This was achieved by embedding pea gravel in the fresh concrete chute surface.

An erodible bed and simulated scour hole erosion were included in the study. Accurate modeling of both of these factors requires a thorough understanding of prototype overburden and bedrock so that the response to hydraulic loading could be determined. Accurate modeling of the material and of its response to the scaled hydraulic forces is also required. This knowledge and modeling ability are difficult to achieve. Consequently, tests were made to obtain qualitative data on bed response and to bracket possible influences of scour hole development. Pea gravel with 0.125-inch (3.2-mm) mean diameter was used to represent the erodible bed. This diameter pea gravel geometrically represents 7.5-inch (190-mm) diameter prototype material. Such material should yield an overestimated prediction of bedrock scour, an underestimated prediction of overburden erosion, and an overestimated prediction of downstream deposition. Model pea-gravel scour and deposition patterns were observed to note tendencies and to bracket possible responses. To evaluate scour hole influences, the observed scour pattern developed with the erodible bed model at a discharge of 125,000 ft³/s (3540 m³/s) was used to define the extent of a scour hole in the bedrock. Although the size of this scour hole is speculation, its shape is representative of the

distribution of hydraulic forces. It was assumed that the maximum depth of this scour hole was sufficient to yield conjugate depth for the 245,000-ft³/s (6940-m³/s) discharge. Thus, the maximum depth is based on the depth at which the hydraulic forces might start to stabilize. It was also noted that the duration of the maximum design discharge was short, less than 12 hours at discharges greater than 20 percent of the maximum design flow. Consequently, it is expected that the extent of the scour hole will be limited. The scour hole as described was installed in the fixed bed of the model and covered with pea gravel up to design grade (fig. 4).

Discharges to the model were set using the laboratory venturi meters. Velocities in the model were measured using propeller and electromagnetic current meters. The reservoir water surface elevation was monitored using a point gauge and stilling well. The tailwater elevation was monitored with a staff gauge, and tailwater wave heights were measured using capacitance wave probes.

THE INVESTIGATION

The initial model was fabricated with fixed bed reservoir and tailwater topography. The waste disposal area at the toe of the dam was not included. Tailwater velocity fields and wave magnitudes were evaluated for discharges of 62,500, 125,000, 187,500, and 245,000 ft³/s (1770, 3540, 5310, and 6940 m³/s), which are approximately 25, 50, 75, and 100 percent of capacity. Velocity and wave data were taken with the tailwater surface elevations at station 354+85, set in accordance with values obtained from a Hydrology Branch tailwater study. The position of the tailwater gauge used is shown on figure 1.

The tailwater gauge elevation settings were 4437.6 feet at 62,500 ft³/s (1352.6 m at 1770 m³/s), 4443.5 feet at 125,000 ft³/s (1354.4 m at 3540 m³/s), 4448.1 feet at 187,500 ft³/s (1355.8 m at 5310 m³/s), and 4451.5 feet at 245,000 ft³/s (1356.8 m at 6940 m³/s). At higher discharges, the water surface at the tailwater gauge was quite rough. Thus, both the theoretically computed tailwater elevation and the set model tailwater elevations had to be approximate averages. With the fixed bed, scour or dissipation holes and deposition bars that could raise the tailwater elevation and increase energy dissipation cannot form. Thus, it was expected that the velocity and wave action observed included minimal energy dissipation and, thus, represent the maximum erosive forces that could be expected. Tailwater velocities measured approximately 7.5 feet (2.3 m) above the bottom represent those to which the bottom surfaces are exposed. The observed velocity fields are shown on figures 5, 6, 7, and 8, and corresponding photographs of these flow conditions are shown on figure 9.

At 62,500 ft³/s (1770 m³/s) [figs. 5 and 9(a)], high tailwater velocities were limited to the stilling basin and the exit channel; the surface roller of the jump was positioned at the chute, and a

drowned jump occurred. The maximum velocities noted in the stilling basin area were approximately 26 ft/s (7.9 m/s). Maximum velocities in the exit channel were approximately 18 ft/s (5.5 m/s). Note also that at a spillway discharge of 62,500 ft³/s (1770 m³/s), the point between the spillway and the outlet works was submerged, but the velocities over the point were low – less than 7.0 ft/s (2.1 m/s). This point is constructed from fill material and, thus, would be subject to erosion. Velocities between the point and the dam embankment were very low, and velocities on the embankment face were less than 1.0 ft/s (0.3 m/s) (fig. 5).

Higher-velocity flow tended to concentrate in a triangular shape in the stilling basin (figs. 5 and 9a). This flow concentration was observed in the stilling basin area for all discharges tested. This flow pattern could be caused either by the flow concentrating to the center of the chute or by inflow from the sides (side eddies) constricting the stilling basin flow (figs. 5 through 9). It was speculated that concentrated flow on the chute might result from either contraction of the flow as it entered the spillway or from “dishing” on the excavated chute surface with boundary friction influences. Long-radius entrance transitions to the crest, which eliminated end contractions, were tested and found to have no effect on the stilling basin flow pattern. It was concluded that entrance conditions influence the crest discharge coefficient but not the tailwater flow pattern. It is thought that the “dishing,” or the curved transition from the chute invert to the excavated sidewalls, with boundary friction losses and the contracting stilling basin flow pattern are the causes of the observed stilling basin flow.

The 125,000-ft³ (3540-m³/s) tailwater flow field shows a similar flow pattern but with higher velocities (figs. 6 and 9b). Again, a drowned hydraulic jump occurs. Maximum observed velocities in the stilling basin area were approximately 52 ft/s (16 m/s), and maximum observed velocities in the exit channel were approximately 19 ft/s (5.8 m/s). Maximum observed velocities over the point were approximately 10 ft/s (3.0 m/s), but maximum observed velocities along the dam embankment were still below 1 ft/s (0.3 m/s).

At 187,500 ft³/s (5310 m³/s), the jump started to sweep out in the portion of the stilling basin with the highest velocity (figs. 7 and 9c). Maximum velocities observed in the stilling basin area were approximately 82 to 86 ft/s (25 to 26 m/s), and maximum velocities in the exit channel were approximately 50 ft/s (15 m/s). Velocities over the point were approximately 15 ft/s (4.6 m/s). Velocities of up to 6 ft/s (2 m/s) were noted between the point and the embankment. Velocities along the dam embankment were still below 1.0 ft/s (0.3 m/s).

Finally, the flow field at 245,000 ft³/s (6940 m³/s) showed an enlarged sweepout zone with higher velocities (figs. 8 and 9d). Maximum velocities in the stilling basin area were approximately 82 to

86 ft/s (25 to 26 m/s), and maximum velocities in the exit channel were 78 ft/s (24 m/s). The eddy over and downstream of the point was large and strong; maximum observed velocities over the point were 15 ft/s (4.6 m/s). Velocities of up to 10 ft/s (3.0 m/s) were noted between the point and embankment, but velocities near the embankment were only about 1.0 ft/s (0.3 m/s).

Wave data were collected along surfaces surrounding the point and along the dam embankment. It was speculated that on some surfaces, wave action may actually be the critical parameter with respect to erosion and protective riprap stability. An eight-channel strip chart recorder was used in conjunction with a matrix of capacitance wave probes to evaluate resulting waves. Data were collected at discharges of 62,500, 125,000, 187,500, and 245,000 ft³/s (1770, 3540, 5310, and 6940 m³/s). Two wave frequencies were noted. A long-period surging was observed in the embayment between the point and the dam. Observed surge periods ranged from 62 to 93 seconds. Maximum trough-to-crest wave magnitudes of up to 5.4 feet (1.6 m) were noted (fig. 10). Although this magnitude is significant, the wave period is so long that the resulting dynamic loading on the riprap is not critical with respect to riprap stability. The most severe long-period surging was observed at a discharge of 187,500 ft³/s (5310 m³/s) (fig. 10). At the maximum discharge, the period shortened (62 to 66 s) and the trough-to-crest magnitude decreased.

A shorter, 11- to 15-second, period surge was observed around the point at the maximum discharge (fig. 10). No surging was observed near the point at the smaller discharges. The maximum discharge surging was associated with the stilling basin flow and the strong eddy that formed to the right of that flow. Trough-to-crest amplitudes of up to 7.5 feet (2.3 m) were observed (fig. 10).

Short, 2- to 4-second, period waves were also observed (fig. 11). These waves were superimposed on the long-period surges. Along the dam embankment, the maximum amplitude of the short-period waves was from 3.3 to 4.5 feet (1.0 to 1.4 m). Maximum amplitudes occurred at discharges of either 245,000 or 187,500 ft³/s (6940 or 5310 m³/s). It is thought that for the dam embankment, the short-period waves caused maximum dynamic loading and, therefore, would be critical with respect to the riprap stability. Waves with a 2- to 4-second period were also observed around and over the point. The highest amplitude (5.6-ft (1.7-m) trough-to-crest) short-period waves at the point occurred at a discharge of 187,500 ft³/s (5310 m³/s). At 245,000 ft³/s (6940 m³/s), trough-to-crest wave amplitudes of approximately 4.7 feet (1.4 m) were observed (fig. 11). Again, these short-period waves were superimposed on the longer-period surges. As previously noted, the period of the long surges over the point was 11 to 15 seconds. This period is short enough that the superimposed long- and short-period waves can yield single random trough-to-crest amplitudes of up to 12 feet (3.7 m). It should be noted that the point was submerged for all discharges tested and, thus, the wave action occurs above, and not on, the point itself.

Deposition of scoured materials could form a downstream bar that would raise the tailwater elevation and modify the tailwater flow patterns. The model tailwater control gate was used to raise the tailwater elevation approximately 10 feet (3.0 m). This was sufficient to establish a drowned jump at the maximum discharge (fig. 12). The higher tailwater increased energy dissipation in the stilling basin area and reduced energy levels, both velocity and wave, in the downstream channel and near the dam embankment. The general flow patterns observed were similar to those observed with the lower tailwater.

The tailwater topography was modified so that the erodible bed tests could be conducted. The potential depth and extent of a scour hole was estimated, and the hole was installed in the fixed bed (fig. 4). In addition, the point previously modeled with fixed topography and the disposal area between the outlet works channel and the dam embankment (fig. 1) were formed with the erodible pea gravel (fig. 13). The disposal area was filled to elevation 4450.0 feet (1356.4 m), which is at or above the tailwater surface elevation for discharges up to 180,000 ft³/s (5100 m³/s). At 245,000 ft³/s (6940 m³/s), the disposal area is submerged approximately 5 feet (1.5 m). It was thought that testing this model arrangement would yield a qualitative evaluation of erosion and deposition patterns, possible flow field modifications caused by the scour and deposition, protection of the dam embankment supplied by disposal material, and the potential for erosion of the dam embankment.

The pea gravel was also placed as a uniform 5-foot (1.5-m) deep overburden on all of the tail box topography. The stilling basin scour hole was brought to design grade, and the point and disposal zone were installed, all using pea gravel. The tailwater was then established using very small spillway discharges to avoid initial scour. With the tailwater set, the initial discharge of 62,500 ft³/s (1770 m³/s) was established and run for an 8-hour prototype duration. During this period, resulting flow field velocities were determined. The model was then shut down, and the resulting erosion and deposition were evaluated. The model was again slowly started up, keeping discharges small to prevent additional erosion until the tailwater was established. With the tailwater established, the discharge was increased to 125,000 ft³/s (3540 m³/s), and the model was again run for an 8-hour prototype duration. Again, flow field velocities were determined and scour and deposition evaluated. This pattern was repeated for discharges of 187,500 and 245,000 ft³/s (5310 and 6940 m³/s). Photographs of the operating conditions are shown on figure 14; tailrace velocities observed are shown on figures 15, 16, 17, and 18; and the deposition and scour patterns observed are shown on figure 19.

As can be seen on figure 19a for the discharge of 62,500 ft³/s (1770 m³/s), a relatively small scour hole with a deposition bar immediately downstream was developed. The depth of the scour

hole was approximately 15 feet (4.6 m), and the height of the deposition bars was approximately 20 feet (6.1 m). A comparison of figures 5 and 15 shows velocities over the point with the erodible bed model to be less than those with the fixed bed model. It appears that the combined scour hole and bar increases energy dissipation and reduces flow velocities in areas away from the stilling basin.

At 125,000 ft³/s (3540 m³/s), the stilling basin or scour hole and the channel bottom downstream of the scour were swept clean to the fixed bed (fig. 19b). No deposition bars that could potentially raise tailwater elevations were formed. Flow over the point eroded a trench approximately 12 feet (3.7 m) deep where the point intersects the hill (fig. 20). A comparison of figures 6 and 16 shows that velocities over the point in the erodible bed model are very similar to those in the fixed bed model. Tailwater elevations were not high enough to submerge the waste pile and, consequently, the pile functioned as protection for the dam embankment.

The 187,500-ft³/s (5310-m³/s) discharge cleaned additional erodible materials from the exit channel (fig. 19c). Again, no bars formed that raised the tailwater. The model tail box included all topography that could potentially influence the tailwater elevation at the dam and spillway. Consequently, indications are that no deposition bars will form where they could influence the tailwater at the dam. Scour continued to deepen the trench at the contact between the point and the hillside (fig. 20). The bottom of the trench was at approximately elevation 4415.0 feet (1345.7 m), the elevation of the fixed bed in the model.

Scour was also noted between the point and the dam embankment near the outlet works stilling basin. This scour was near the intersection between the dam embankment and the left abutment. As can be seen on figure 17, velocities between 15 and 20 ft/s (4.6 and 6.1 m/s) were noted in this area. Flow at these velocities also eroded the waste area and passed over the point; however, the waste pile was not submerged. Comparison of these velocities with those observed for the fixed bed model (figs. 7 and 17) showed considerably higher velocities in the erodible bed model. Apparently, erosion of the point allows more circulation, which increases velocities in the embayment between the point and the dam. The higher velocities are more representative of what would occur in the prototype. Significant erosion of the waste area pile occurred during the 8-hour (prototype) test. However, much of the waste area remained at completion of the test, indicating that the waste material supplied ample protection to the embankment at the 187,500-ft³/s (5310-m³/s) discharge.

The 245,000 ft³/s (6940 m³/s) discharge swept more of the overburden from the fixed topography (fig. 19d). The eroded trench through the point was somewhat enlarged, but was no deeper since

the scour had reached the fixed surface topography. A large bar to the right of the spillway stilling basin continued to grow. This bar, which is a portion of the point with additional deposition, lies under the center of a large eddy that forms to the right of the stilling basin and the exit channel (fig. 18). This bar evolved with increasing discharge and had no influence on tailwater elevations. Additional scour of the waste pile occurred, but a portion of the waste pile remained over the entire embankment face. Again, this indicates that the waste pile should supply good protection to the embankment. A comparison of figures 8 and 18 shows that velocities in the eddy between the spillway and the dam were much higher in the erodible bed model than in the fixed bed model. Velocities observed along the waste pile were between 10 and 20 ft/s (3.0 and 6.1 m/s). Velocities through the trench were as high as 26 ft/s (7.9 m/s) (fig. 18). As previously noted, the velocities observed in the erodible bed model reflect increased circulation that would result from erosion of the point. It is thought that the results of the erodible bed model better reflect velocities that will occur in the prototype. At the 245,000-ft³/s (6940-m³/s) discharge, the tailwater surface elevation of approximately 4455.0 feet (1357.9 m) at the embankment face was above the top of the waste pile. The water depth over the waste pile was shallow, approximately 5 feet (1.5 m), and hydraulic forces transferred from the main eddy to the embankment were small. Maximum observed velocities on the dam embankment face were less than 10 ft/s (3.0 m/s) and were generally less than 5 ft/s (1.5 m/s) (fig. 18). Velocities on the eroding face of the waste area were, however, considerably higher; observed velocities ranged from 9.0 to 18.9 ft/s (2.7 to 5.8 m/s). Long-period surges did not occur near the embankment, and a large-diameter stable eddy rotated over the point. Short-period wave amplitudes at the dam embankment were minimal. Maximum wave amplitudes over the point were approximately 5 feet (1.5 m) and were observed at discharges of 125,000 and 245,000 ft³/s (3540 and 6940 m³) (fig. 21).

Even though it appears that high tailwater elevations caused by downstream bar formation are unlikely, the performance of the erodible bed model with an artificially raised tailwater was observed. The model tailwater control gate was used to artificially raise the tailwater elevation for the 245,000-ft³/s (6940-m³/s) discharge from elevation 4455.0 feet (1357.9 m) to elevation 4465.0 feet (1360.9 m). It was noted that, as with the fixed bed model, the elevated tailwater increased energy dissipation in the stilling basin and, thus, reduced flow velocities and wave action downstream of the stilling basin and in the embayment.

The reservoir approach flow conditions to the crest and the crest discharge rating were also studied. In the early phases of this design development, a 1:36 scale sectional model of the crest was constructed to determine discharge coefficients for the crest over an extended head range and for various depths of approach channel. Of particular concern was the shallow approach that exists at the Pactola site. The sectional model yielded appropriate coefficients for the center portion

of the crest. It did not, however, consider end effects or end contractions (fig. 22). Discharge coefficients obtained from the two models are shown on figure 23. Note that agreement is generally good, but that at higher discharges, the coefficients from the 1:60 model tend to be lower than the coefficients from the 1:36 model. This reflects the influence of the end contractions (fig. 22) that occur in the full structure model. A discharge rating curve for the crest that corresponds to the 1:60 model coefficients curve is shown on figure 24.

The magnitude of reservoir approach velocities to the crest was evaluated to determine whether there was a need for protective surfacing in the reservoir. As can be seen on figure 25, a dike extends from the existing ground surface, which is at approximately elevation 4640.0 feet (1414.3 m), to the new dam crest elevation of 4655.0 feet (1418.8 m). The reservoir topography thus includes a benched reach of natural ground surface at approximately elevation 4640.0 feet (1414.3 m) with a 0.5:1 cut down to the highway road surface. The elevation of the road surface varies, ranging from approximately 4630.0 feet (1411.2 m) to 4620.0 feet (1408.2 m). Velocities were measured 3 feet (1.0 m) above the topography surface for the 245,000-ft³/s (6940-m³/s) discharge. The observed velocity field is shown on figure 26.

As shown on figure 26, the flow accelerates as it approaches the spillway structure. Velocities over the higher ground to the left of the spillway range from 5.5 to 12 ft/s (1.7 to 3.7 m/s), although those over most of the area range from 8 to 11 ft/s (2.4 to 3.4 m/s). The water is deeper to the right of the spillway and, consequently, the velocities are lower. These velocities observed ranged from 3 to 12 ft/s (0.9 to 3.7 m/s), and most of the surface was exposed to velocities in the 3- to 7-ft/s (0.9- to 2.1-m/s) range. On both sides, localized higher-velocity areas occur in the flow contraction zones near the spillway retaining walls (fig. 26). These areas, along with the invert of the approach channel, are the ground surfaces exposed to the highest velocities. Velocities as high as 25 to 30 ft/s (7.6 to 9.1 m/s) are possible over these flow surfaces. As shown on figure 1 in the final design, protective surfacing was placed on the right cut slope approach to the crest to prevent erosion in this area.

APPENDIX

After completion of the model study and removal of the model from the laboratory, construction on the prototype structure showed that little waste material was available to construct the proposed waste pile at the toe of the dam. Consequently, the flow-modifying influence and embankment erosion protection offered by such a waste pile will not be available.

To address the potential impact of the waste pile exclusion, the findings presented in this report were reviewed. Wave height and velocity data at the embankment face obtained with the fixed

bed model should be conservative, and representative of design hydraulic forces for discharges up to 125,000 ft³/s (3540 m³/s). These values are conservative because the fixed bed model did not include a scour hole at the toe of the spillway chute and, thus, underestimates energy dissipation. These findings indicate that for discharges of 125,000 ft³/s (3540 m³/s) or less, velocities on the embankment face would be near zero and that short-period waves with maximum trough-to-crest magnitudes of approximately 2 feet (0.6 m) can be expected. At higher discharges, the point between the stilling basins erodes; this modifies flow patterns near the embankment. Consequently, for discharges greater than 125,000 ft³/s (3540 m³/s), velocities on the embankment face are expected to be greater than those indicated by the fixed bed model. Because the waste pile reduces the size of the embayment, velocities at the embankment are expected to be less than those observed along the waste pile face in the erodible bed model. Note that the waste pile eroded during the tests and substantially decreased in size. Thus, the velocity and wave data obtained from the erodible bed model, although conservative, probably represent the most appropriate available information for the design of embankment protection for discharges greater than 125,000 ft³/s (3540 m³/s). These data indicate maximum velocities along the embankment face of 19 ft/s (5.8 m/s) with minimal wave magnitudes.

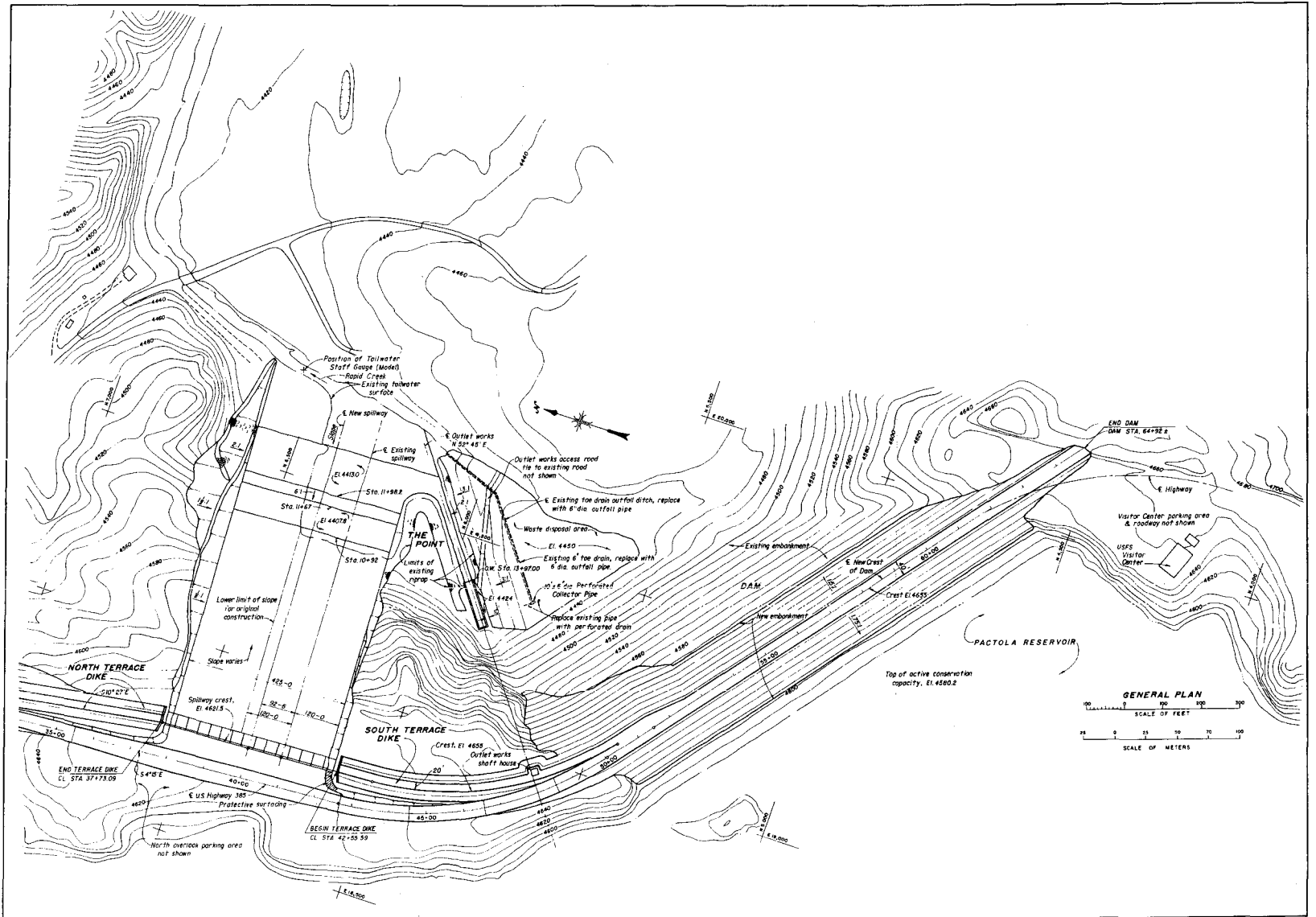
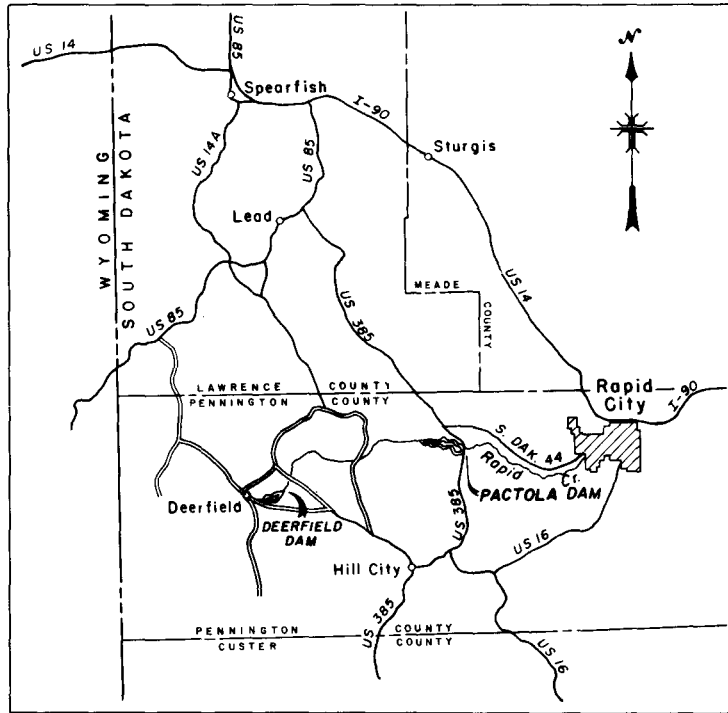
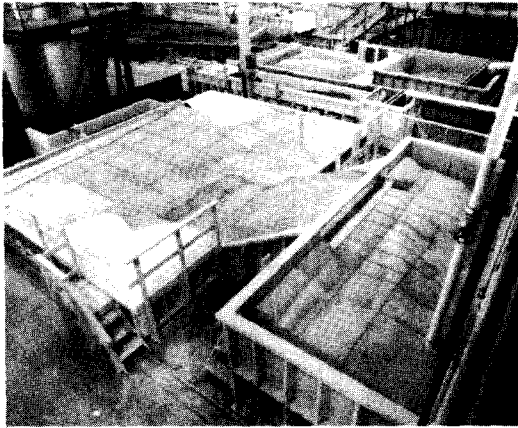


Figure 1. - General plan of Pactola Dam and spillway.

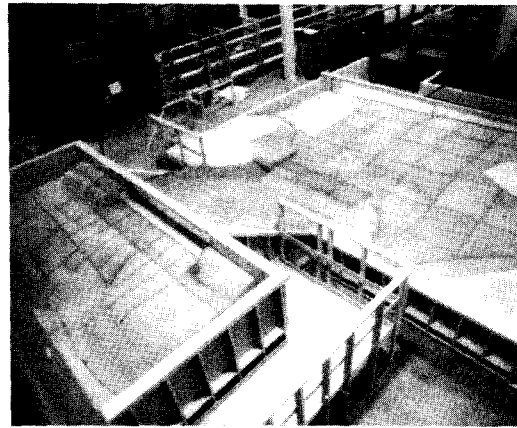


KEY MAP

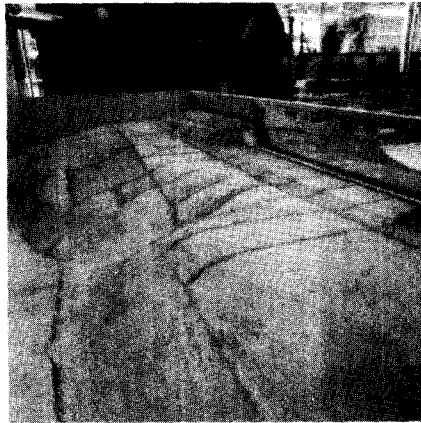
Figure 2. – Location map.



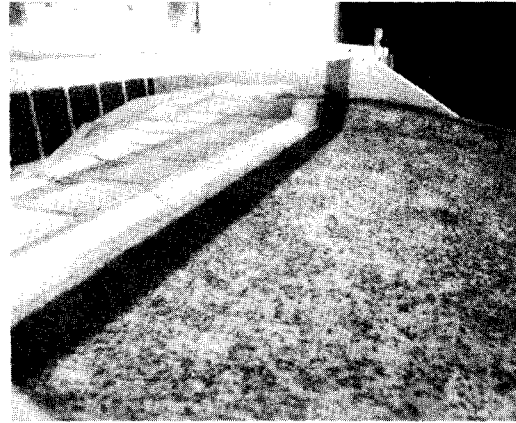
a. View of model from rear-left.



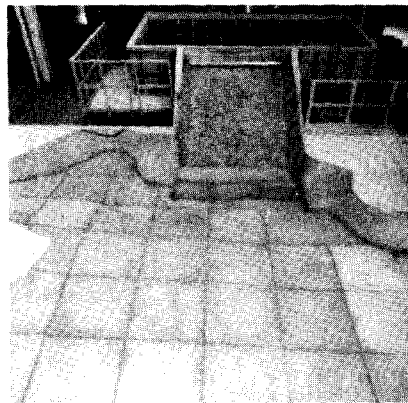
b. View of model from rear-right.



c. Reservoir topography and spillway crest.

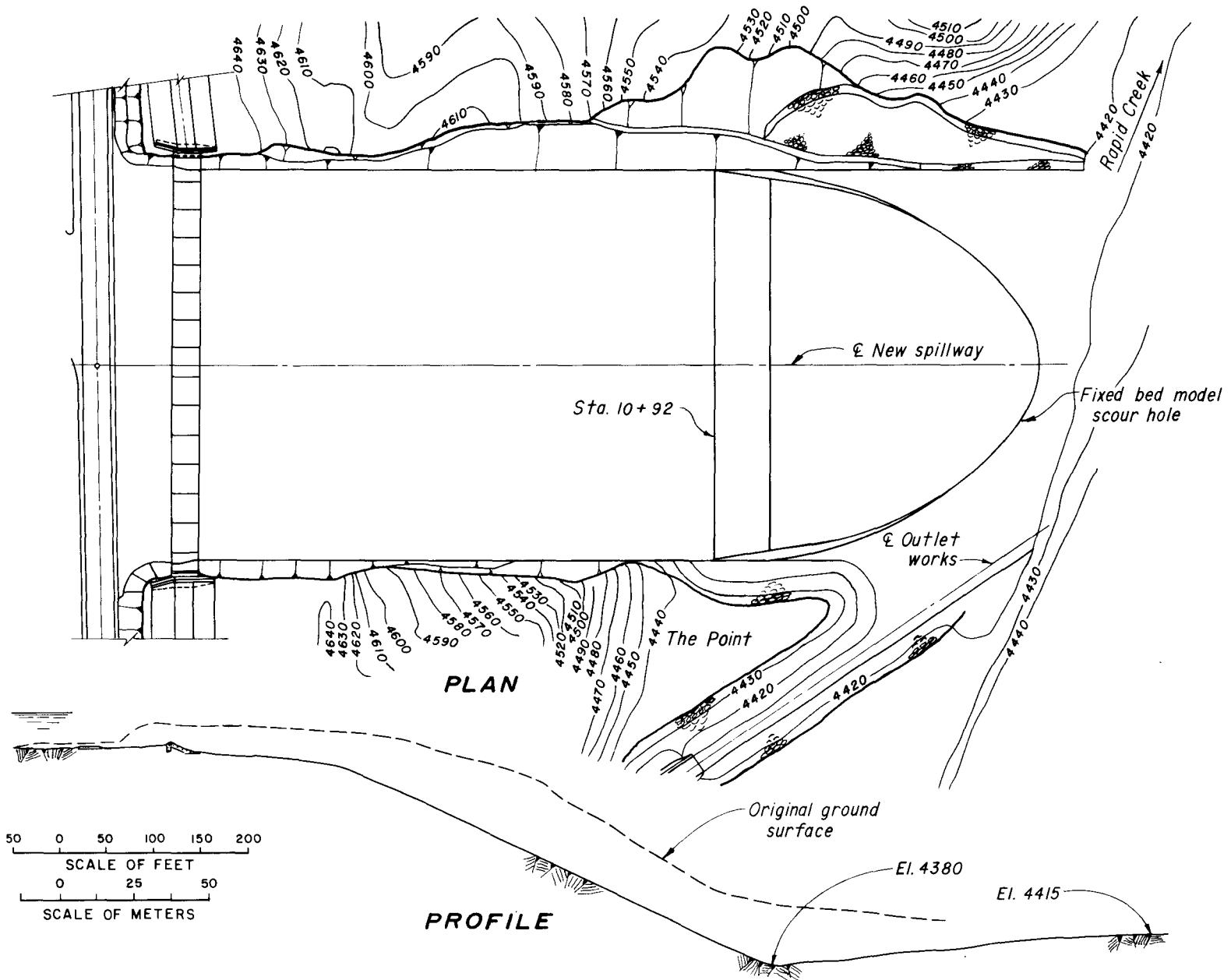


d. Spillway crest and upper chute.



e. Tailwater topography and spillway chute.

Figure 3. – Hydraulic model, 1:60 scale.



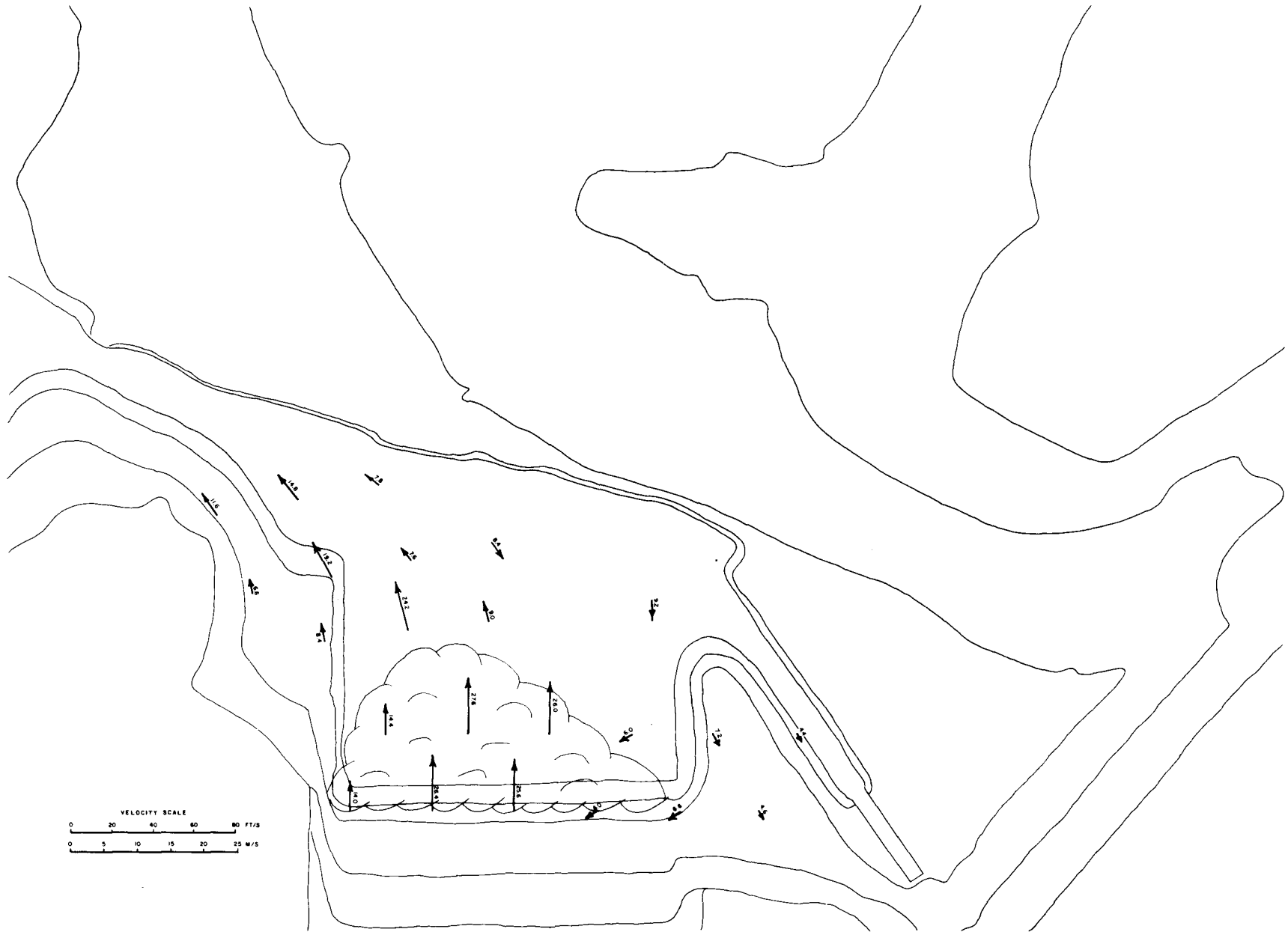


Figure 5. – Fixed bed tailwater velocity distribution for discharge of 62,500 ft³/s (1770 m³/s). Velocities shown are in feet per second.

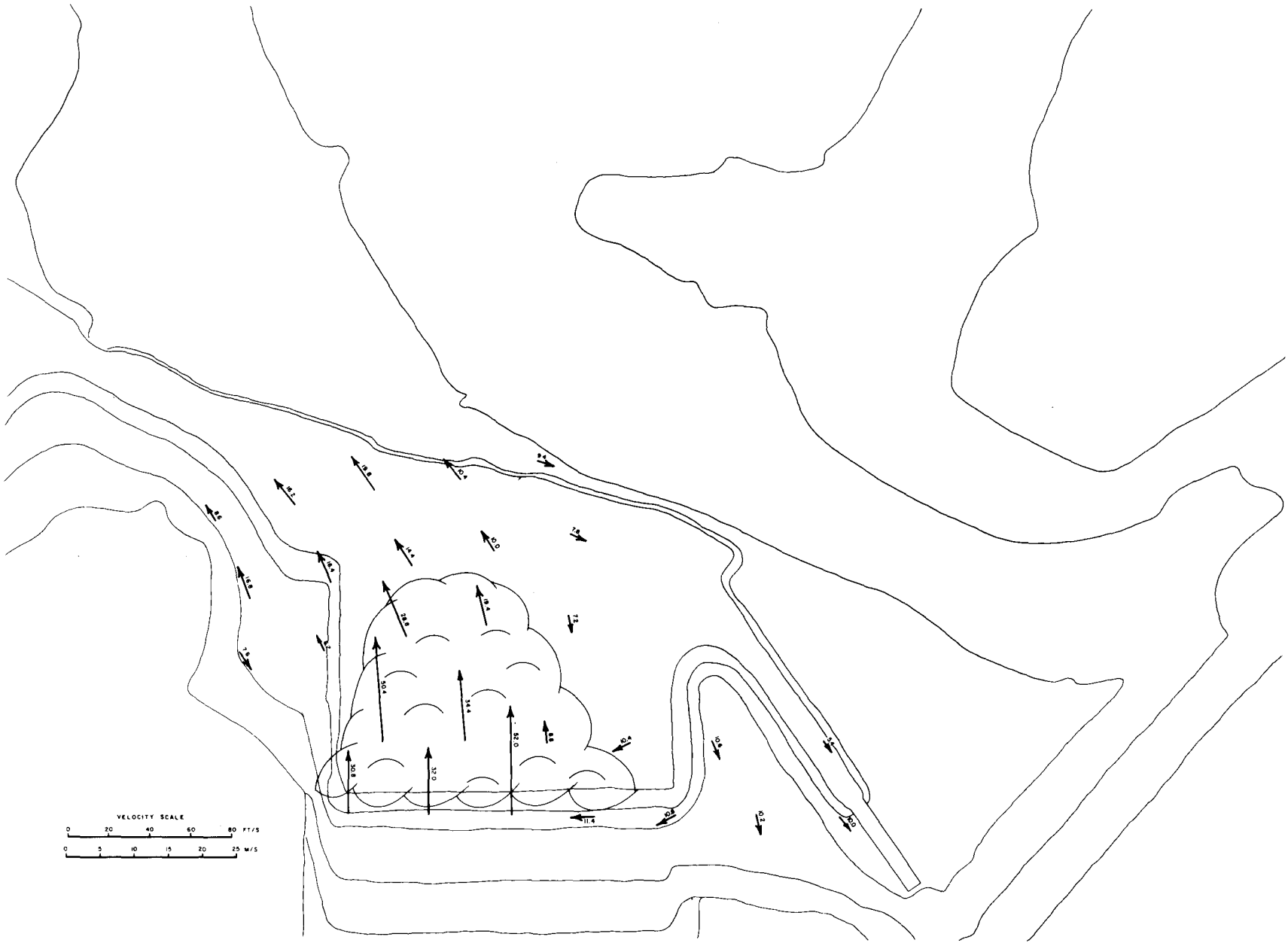


Figure 6. – Fixed bed tailwater velocity distribution for discharge of 125,000 ft³/s (3540 m³/s). Velocities shown are in feet per second.

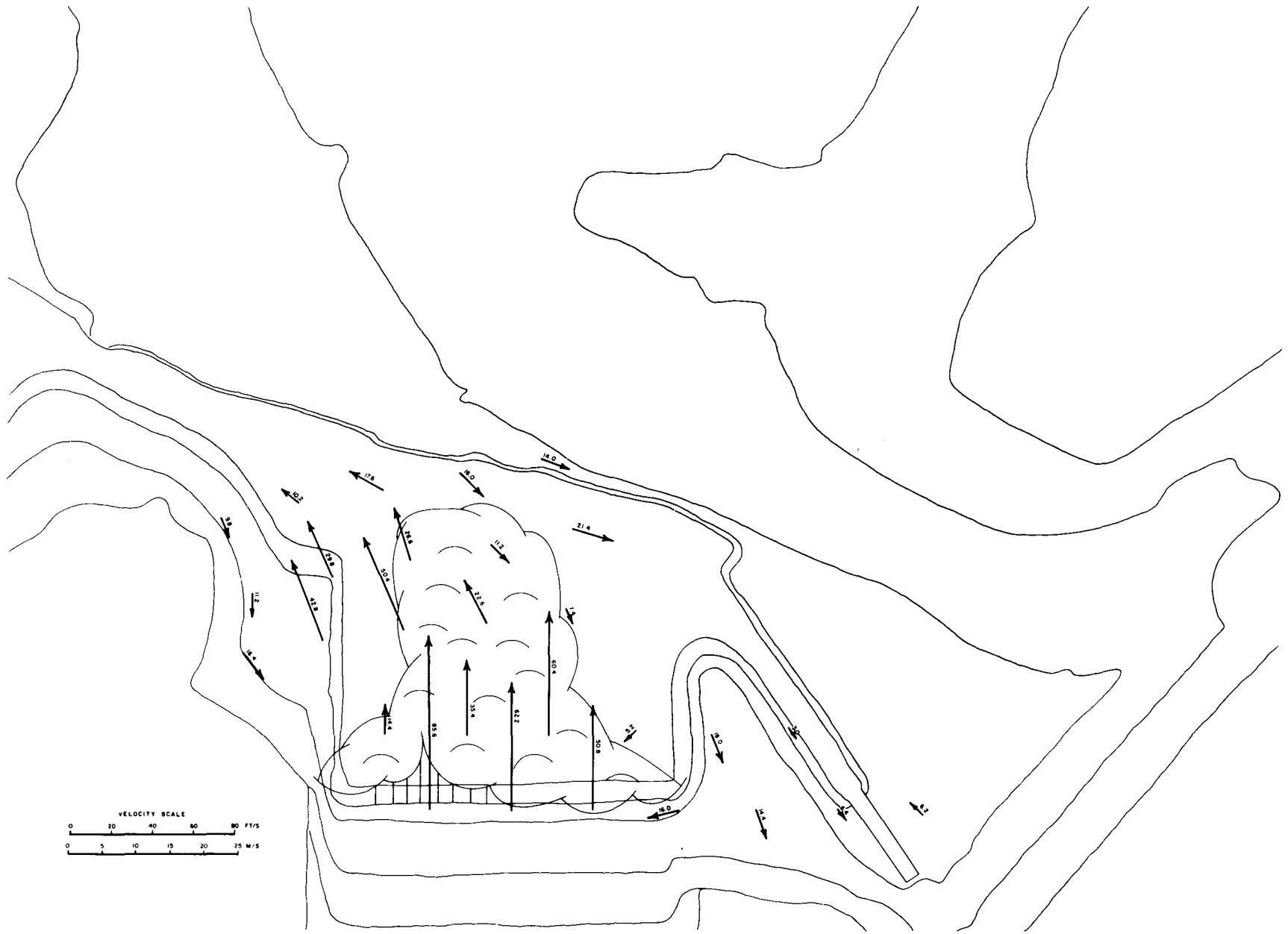
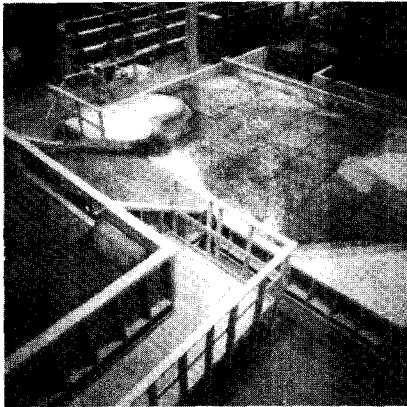


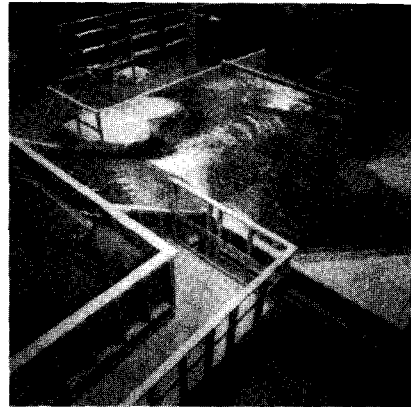
Figure 7. – Fixed bed tailwater velocity distribution for discharge of 187,500 ft³/s (5310 m³/s). Velocities shown are in feet per second.



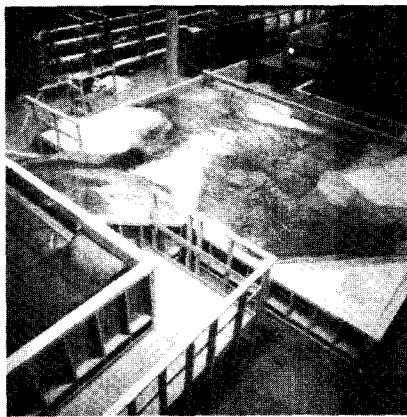
Figure 8. – Fixed bed tailwater velocity distribution for discharge of 245,000 ft³/s (6940 m³/s). Velocities shown are in feet per second.



a. 62,500 ft³/s (1770 m³/s).



b. 125,000 ft³/s (3540 m³/s).



c. 187,500 ft³/s (5310 m³/s).



d. 245,000 ft³/s (6940 m³/s).

Figure 9. – Fixed bed hydraulic model at various discharges.

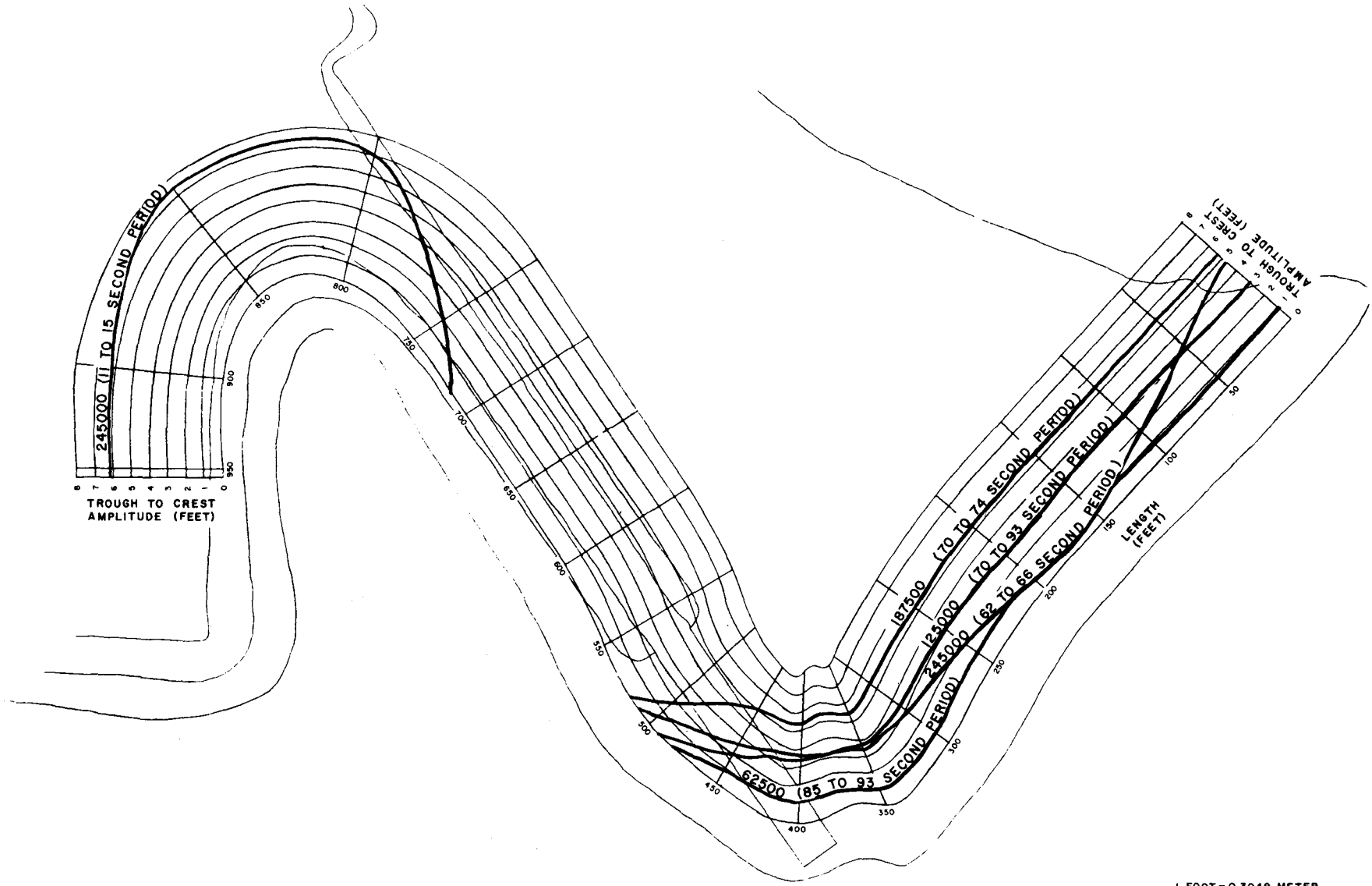
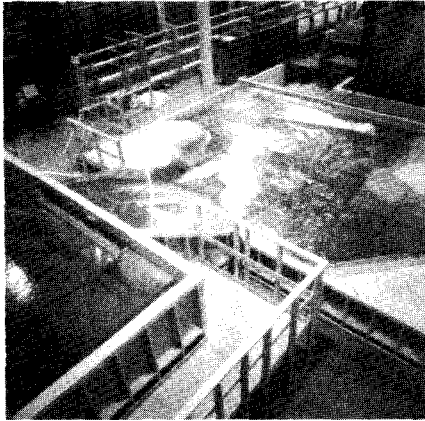


Figure 10. - Fixed bed, long-period maximum observed wave amplitudes.

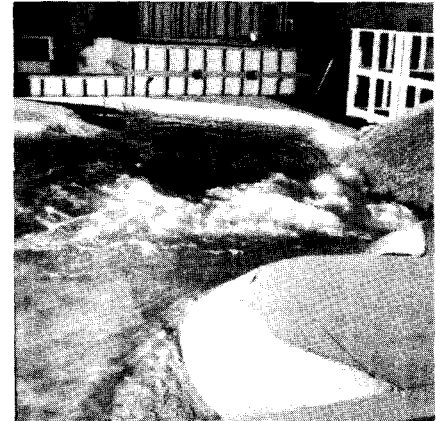
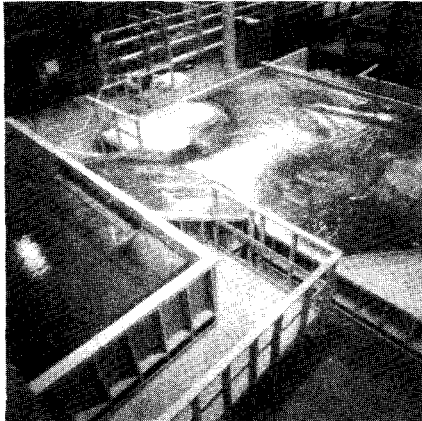
1 FOOT = 0.3048 METER



Figure 11. - Fixed bed, short-period (2- to 4-s) maximum observed wave amplitudes.



a. Predicted tailwater elevation.



b. Tailwater artificially elevated 10 feet (3 m).

Figure 12. – Influence of high tailwater on fixed bed flow for discharge of 245,000 ft³/s (6940 m³/s).

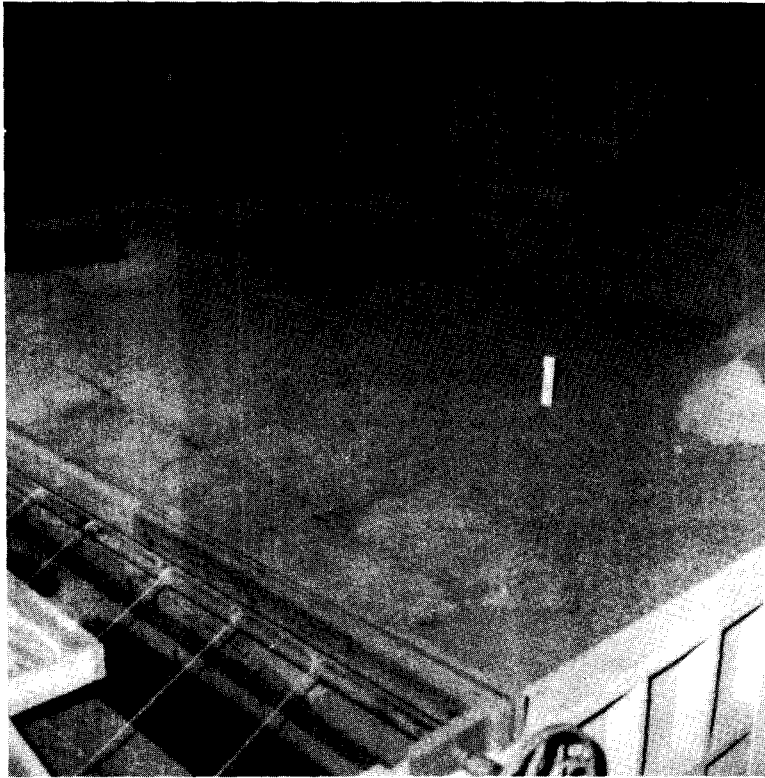
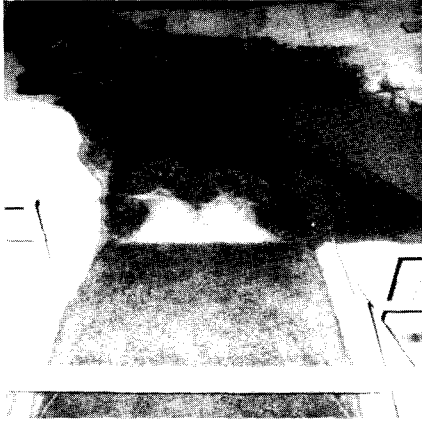


Figure 13. – Model with erodible bed.



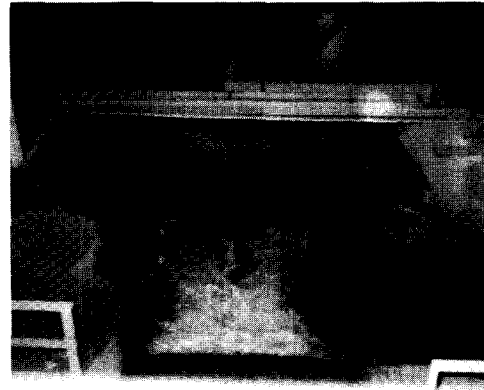
a. 67,500 ft³/s (1770 m³/s).



b. 125,000 ft³/s (3540 m³/s).



c. 187,500 ft³/s (5310 m³/s).



d. 245,000 ft³/s (6940 m³/s).

Figure 14. – Operation of model with erodible bed at various discharges.

30

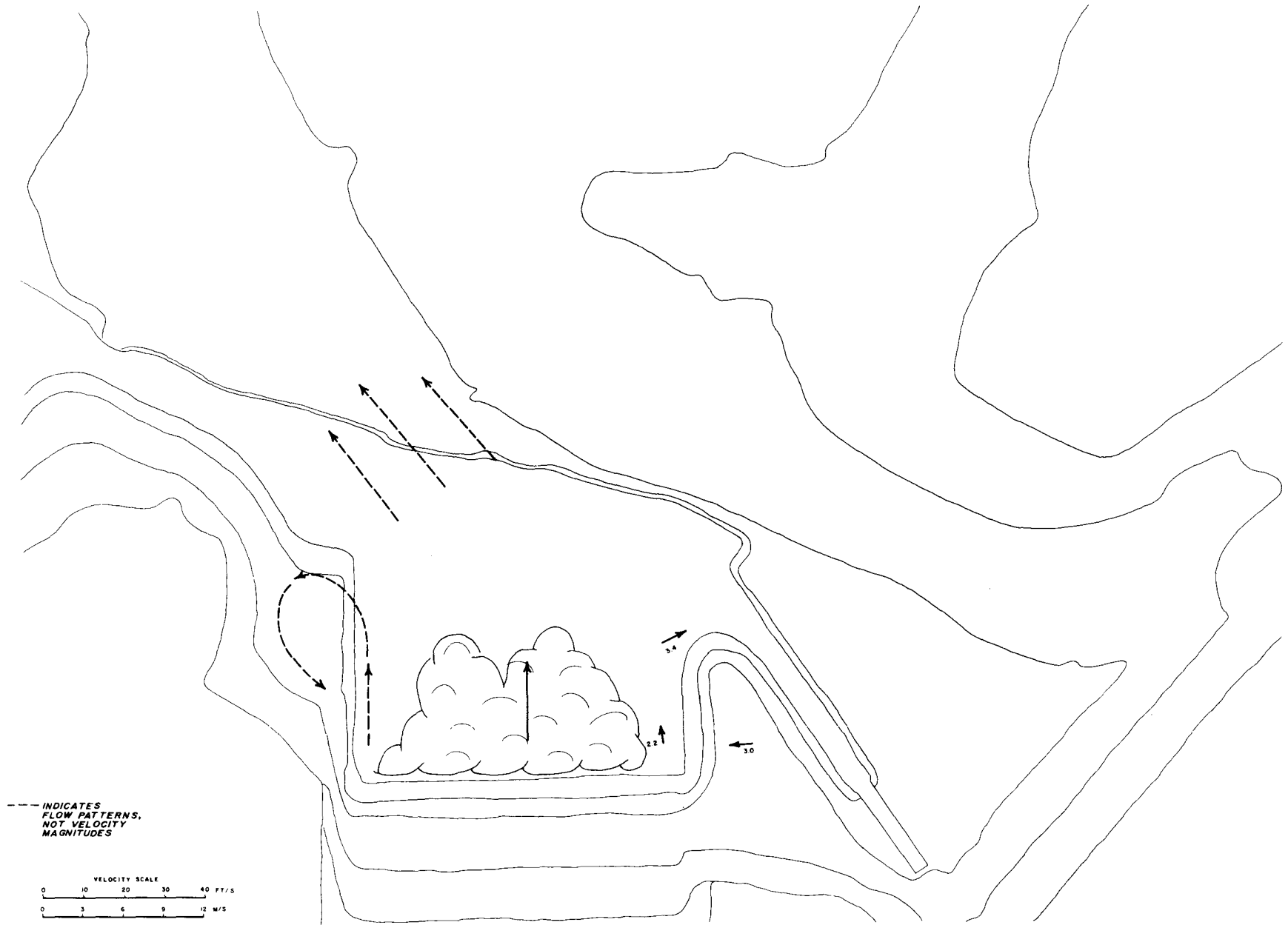


Figure 15. – Erodible bed tailwater velocity distribution for discharge of 62,500 ft³/s (1770 m³/s). Velocities shown are in feet per second.

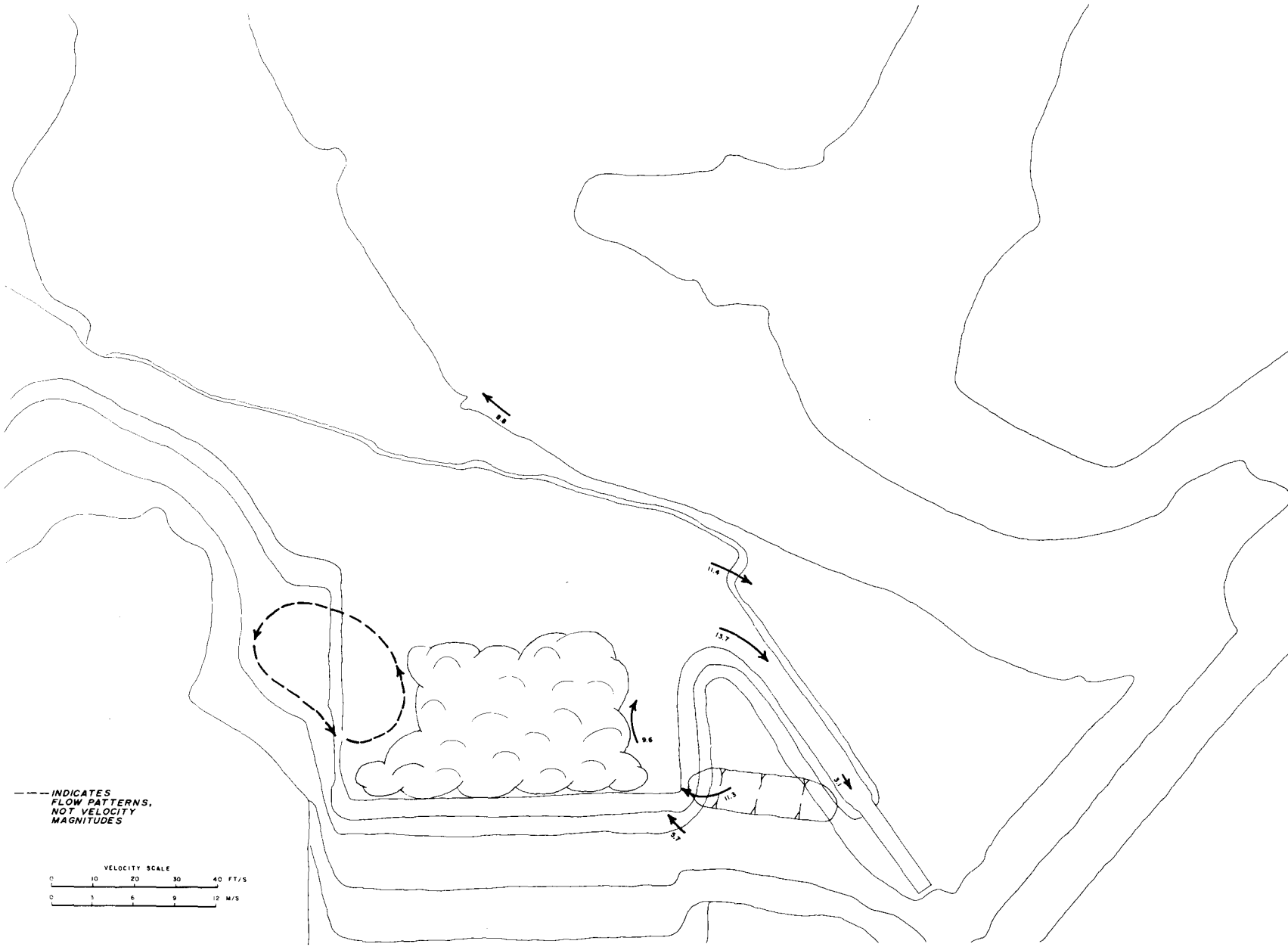


Figure 16. – Erodible bed tailwater velocity distribution for discharge of 125,000 ft³/s (3540 m³/s). Velocities shown are in feet per second.



Figure 17. - Erodeable bed tailwater velocity distribution for discharge of 187,500 ft³/s (5310 m³/s). Velocities shown are in feet per second.

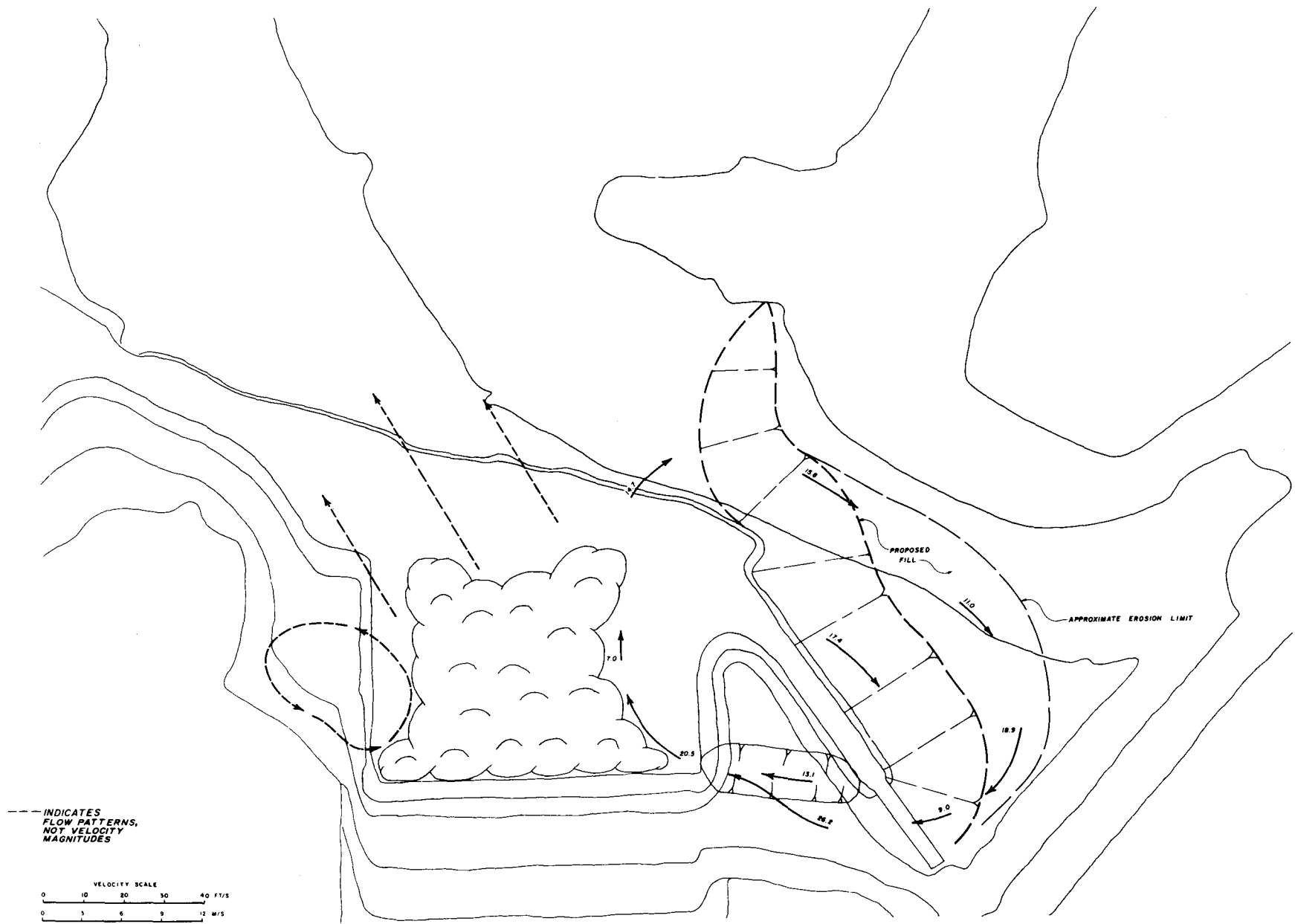
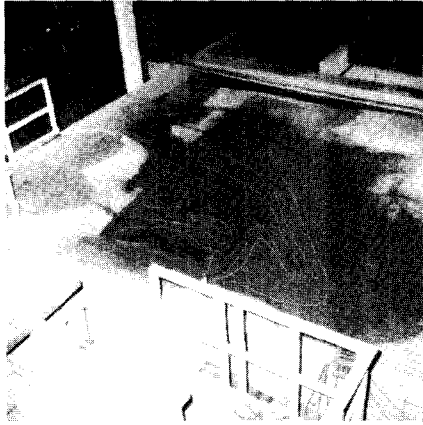


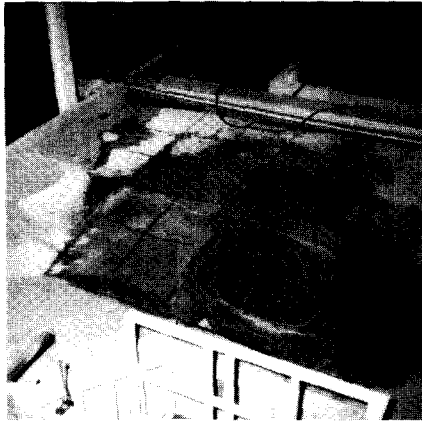
Figure 18. – Erodible bed tailwater velocity distribution for discharge of 245,000 ft³/s (6940 m³/s). Velocities shown are in feet per second.



a. 62,500 ft³/s (1770 m³/s).



b. 125,000 ft³/s (3540 m³/s).



c. 187,500 ft³/s (5310 m³/s).



d. 245,000 ft³/s (6940 m³/s).

Figure 19. – Erodible bed scour at various discharges.

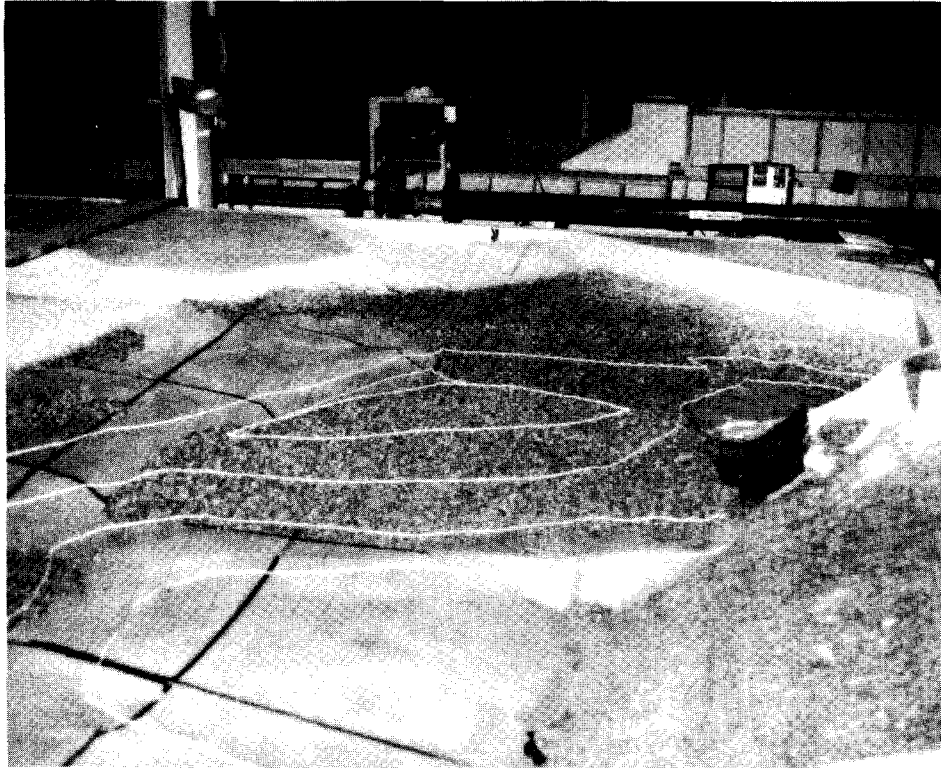


Figure 20. – Point erosion with deposition bar for discharge of $245,000 \text{ ft}^3/\text{s}$ ($6940 \text{ m}^3/\text{s}$).

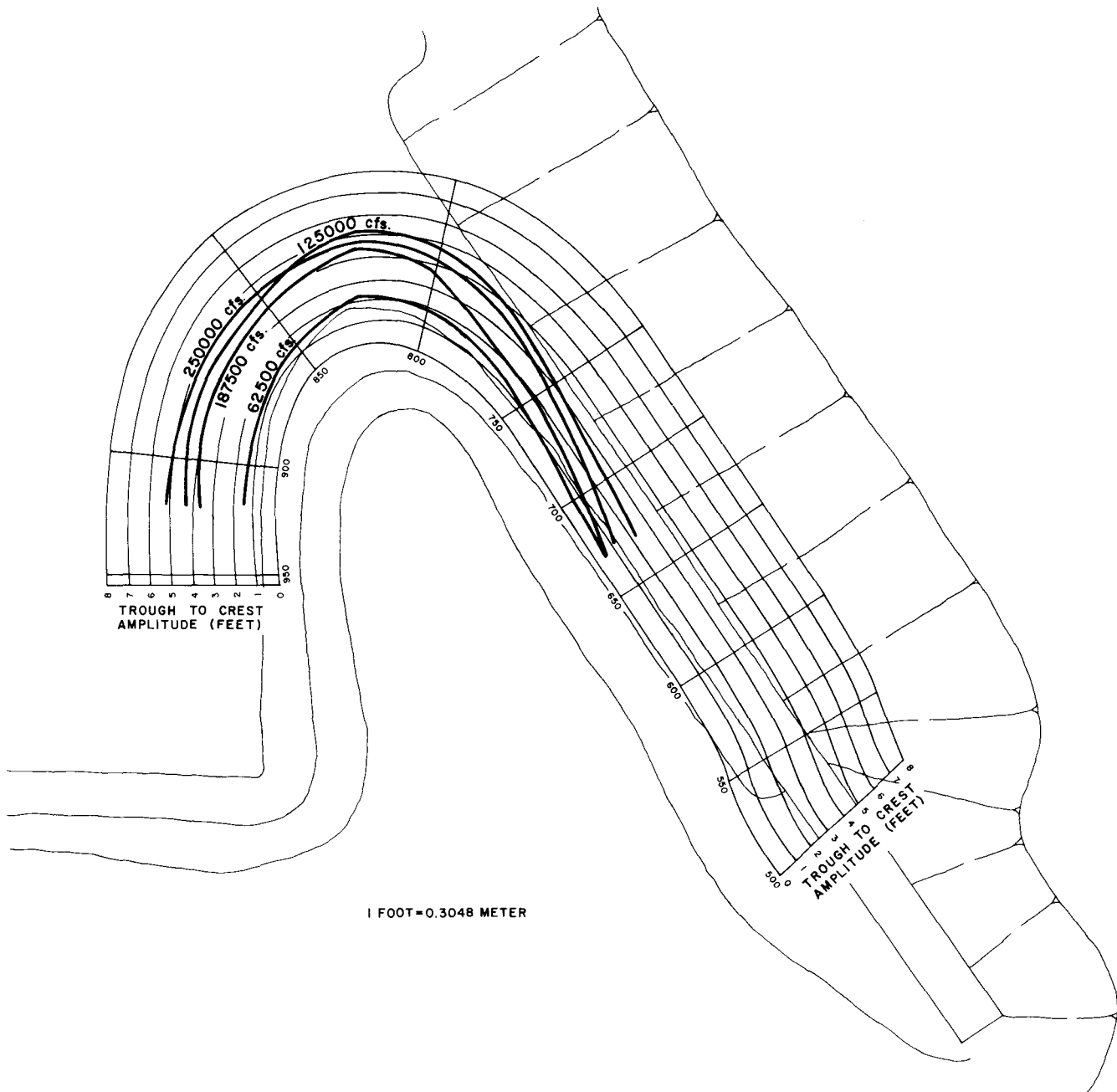


Figure 21. – Erodible bed maximum observed wave amplitudes over point.

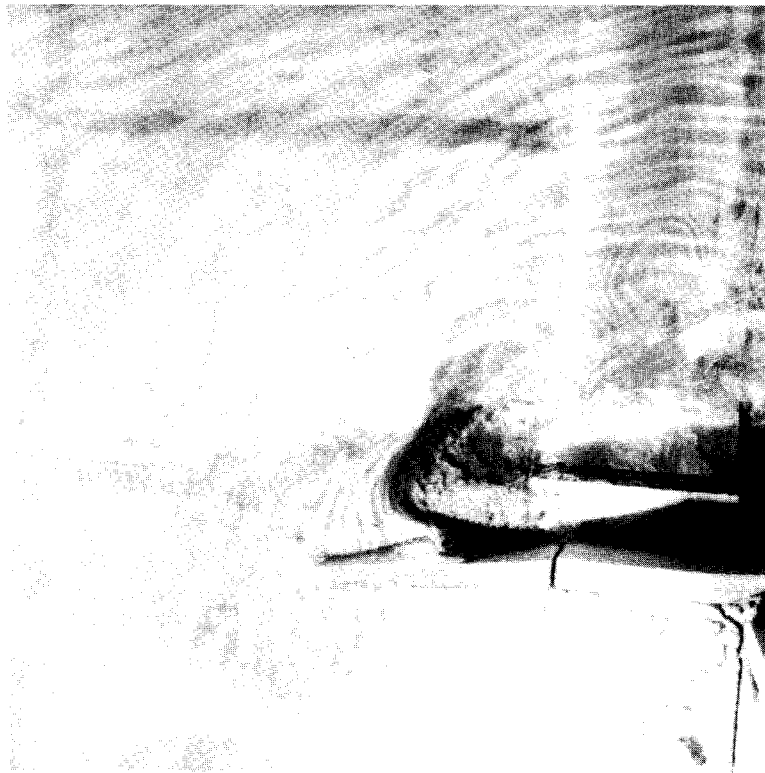


Figure 22. – End contraction of flow at crest.

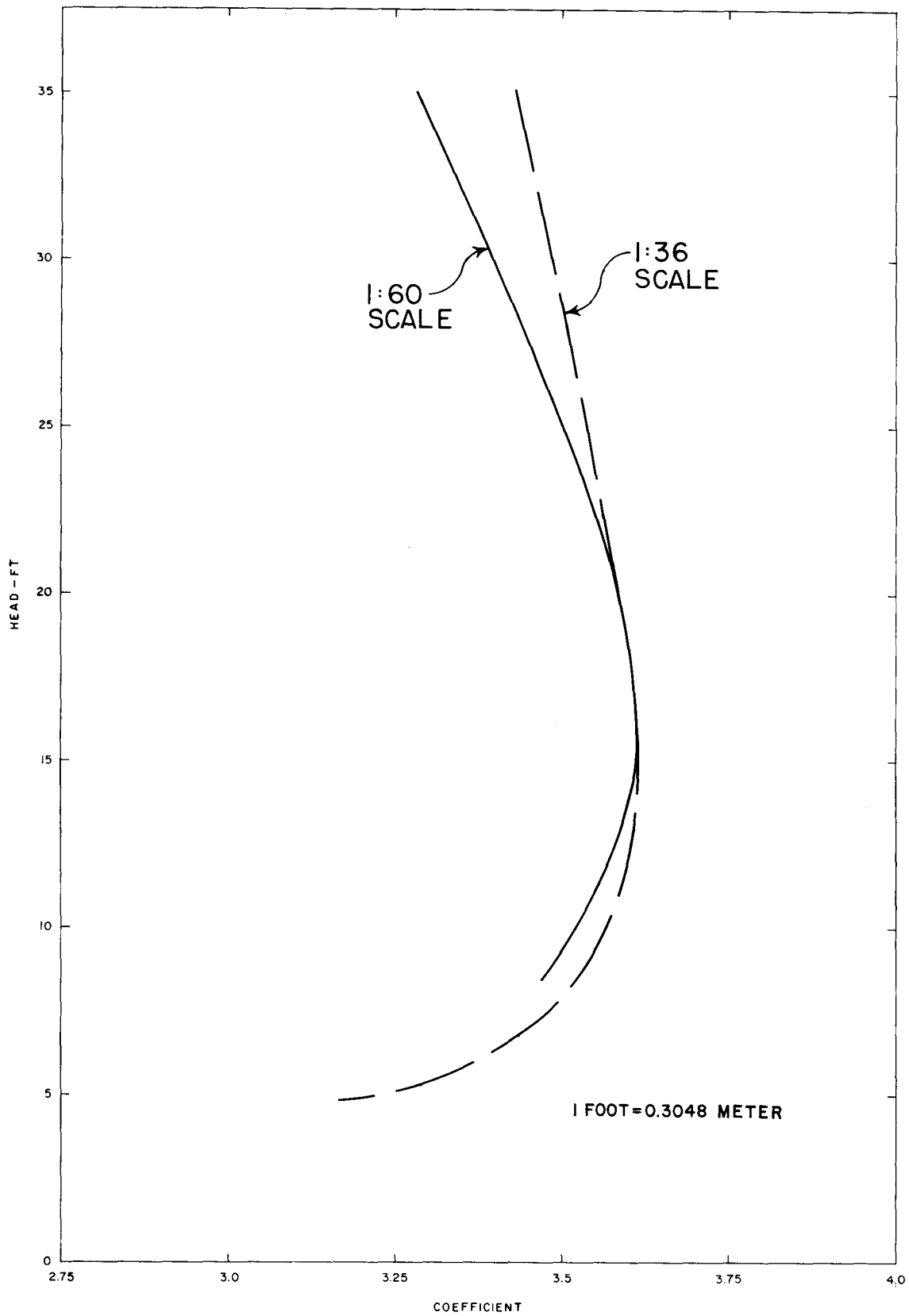


Figure 23. - Crest discharge coefficients from 1:60 and 1:36 scale models.

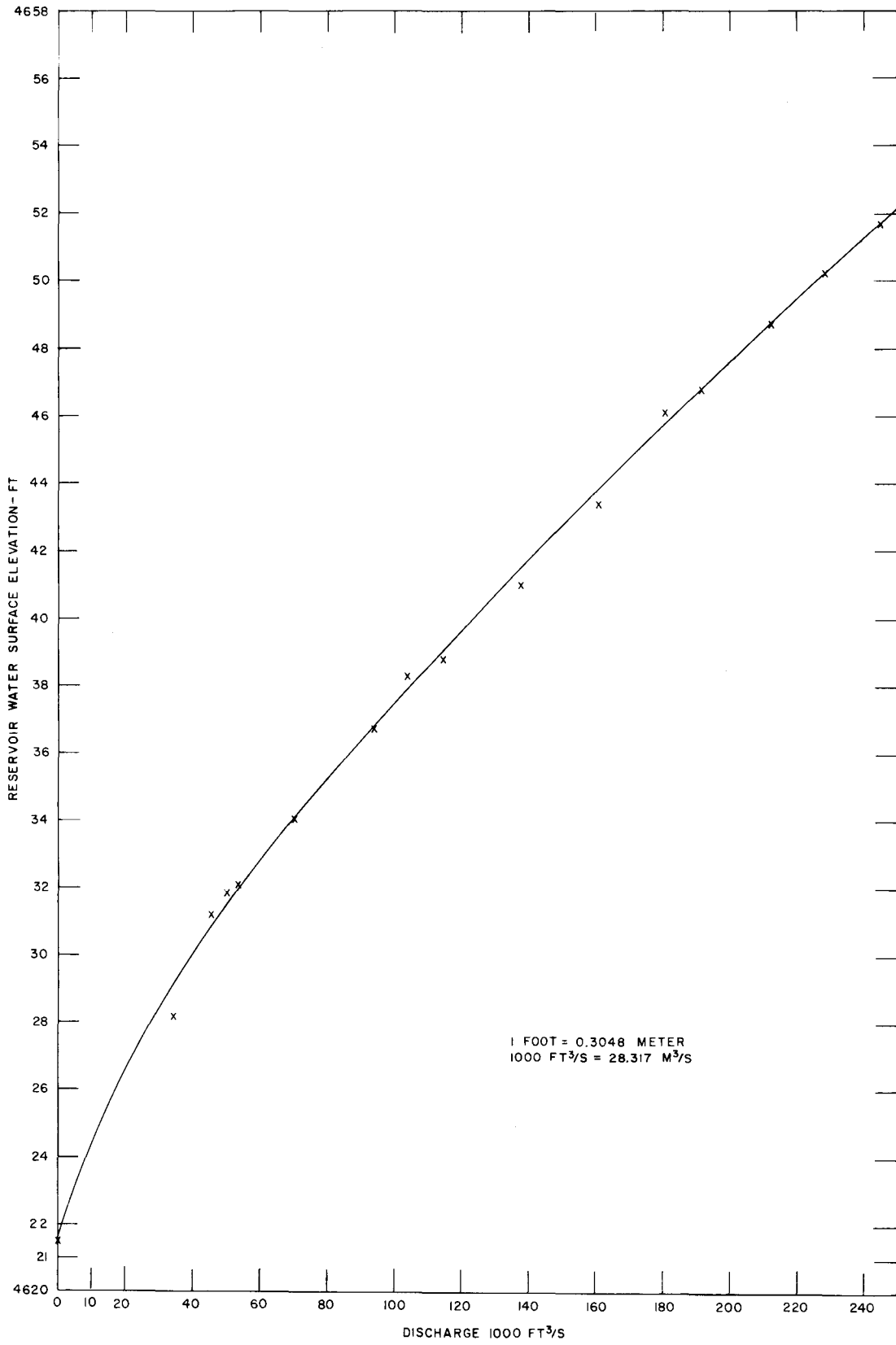


Figure 24. - Discharge rating curve.

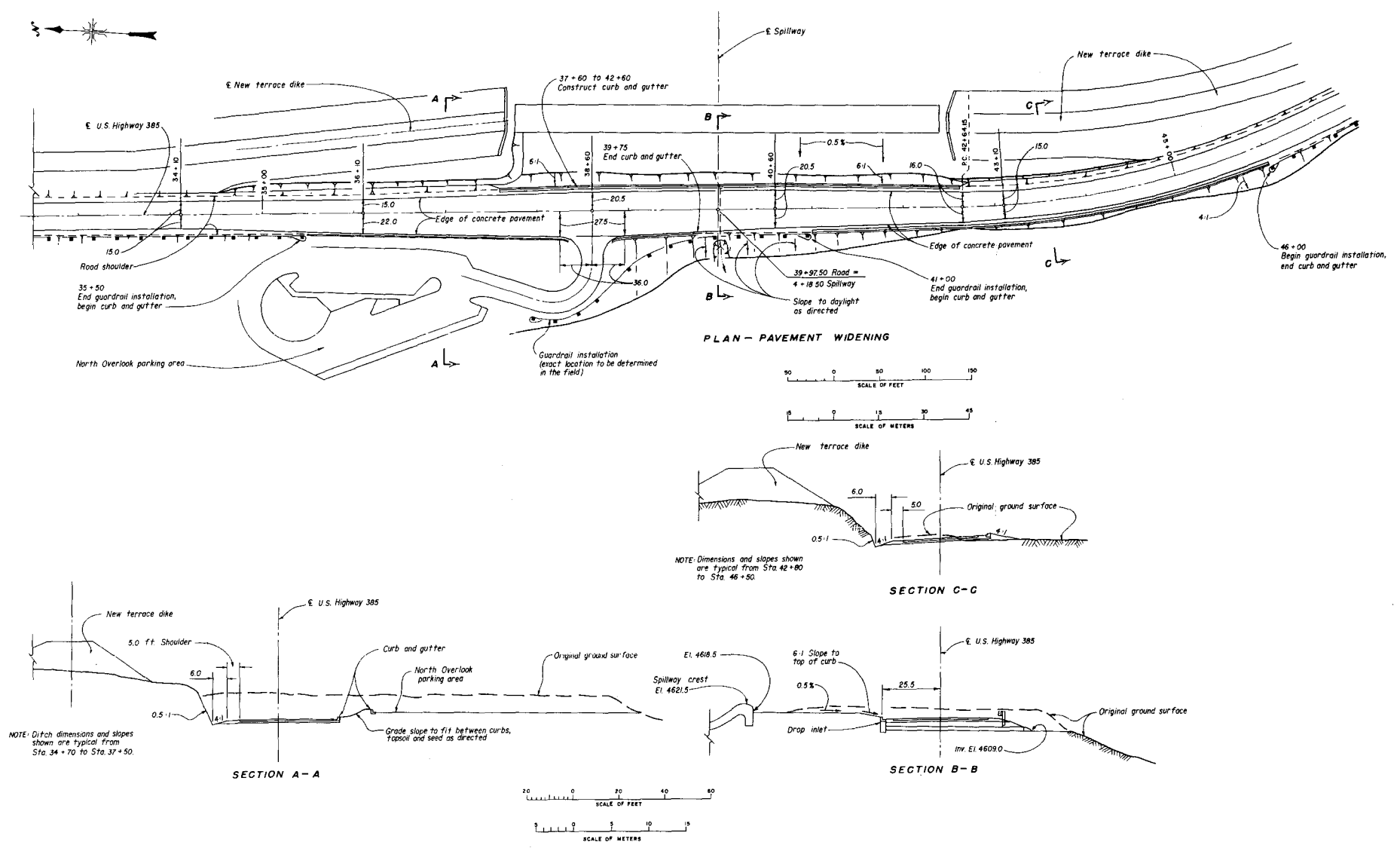


Figure 25. - Topography at spillway intake. 494-D-200.

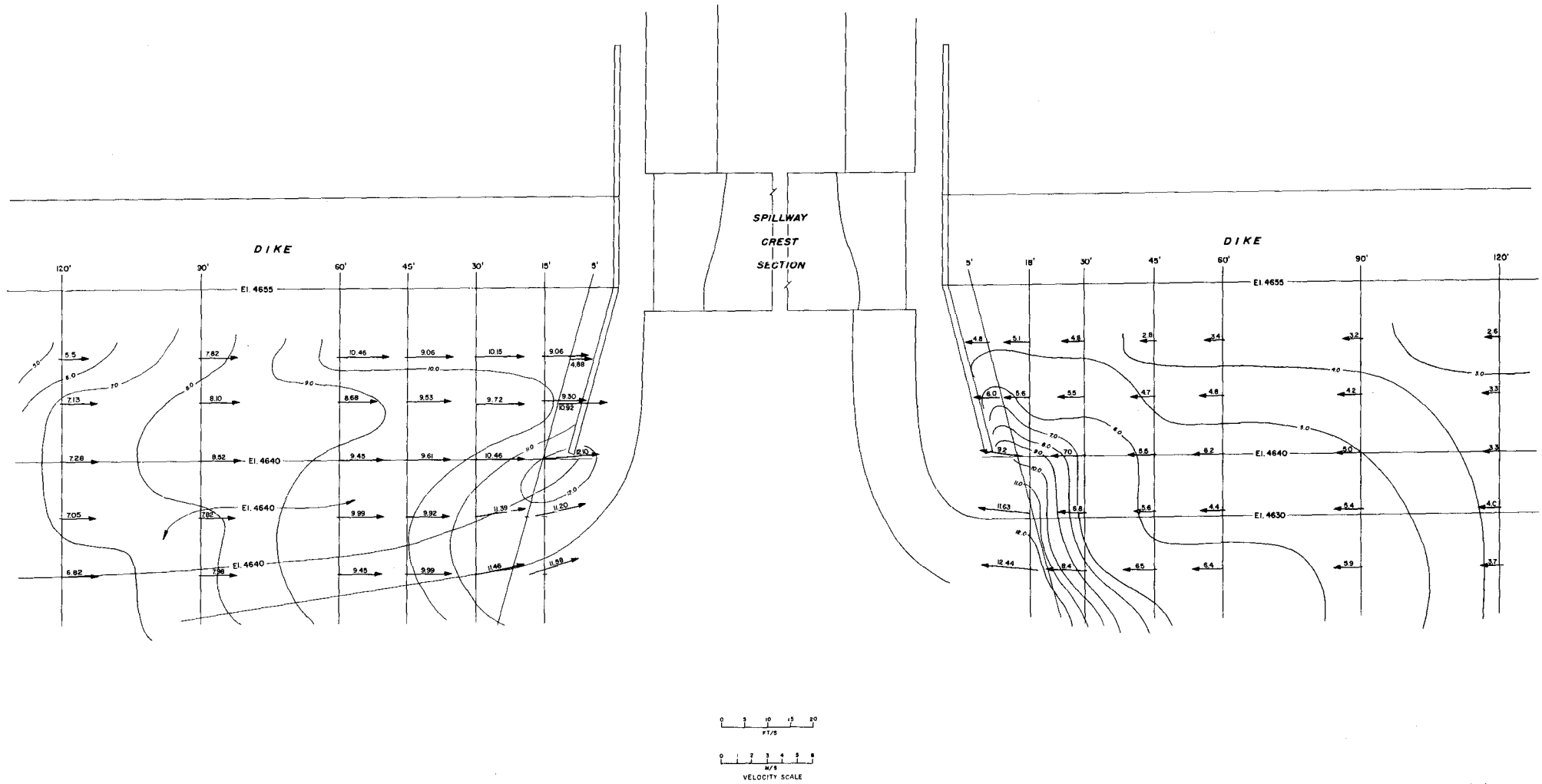


Figure 26. - Velocity distribution in reservoir approach to spillway for discharge of 245,000 ft²/s (6940 m²/s). Velocities shown are in feet per second.

Mission of the Bureau of Reclamation

The Bureau of Reclamation of the U.S. Department of the Interior is responsible for the development and conservation of the Nation's water resources in the Western United States.

The Bureau's original purpose "to provide for the reclamation of arid and semiarid lands in the West" today covers a wide range of interrelated functions. These include providing municipal and industrial water supplies; hydroelectric power generation; irrigation water for agriculture; water quality improvement; flood control; river navigation; river regulation and control; fish and wildlife enhancement; outdoor recreation; and research on water-related design, construction, materials, atmospheric management, and wind and solar power.

Bureau programs most frequently are the result of close cooperation with the U.S. Congress, other Federal agencies, States, local governments, academic institutions, water-user organizations, and other concerned groups.

A free pamphlet is available from the Bureau entitled "Publications for Sale." It describes some of the technical publications currently available, their cost, and how to order them. The pamphlet can be obtained upon request from the Bureau of Reclamation, Attn D-822A, P O Box 25007, Denver Federal Center, Denver CO 80225-0007.